Multifaceted analysis reveals diet and kinship of Late Pleistocene “Tumat Puppies”

Anne Kathrine Wiborg Runge[1,2], Jonas Niemann[1,2], Mietje Germonpré[3], Dorothée G. Drucker[4], Hervé Bocherens[4,5], Kseniia Boxleitner[6], Jazmín Ramos-Madrigal[2,7], Anna Linderholm[8,9], David W. G. Stanton[8, 9, 10, 11,12], Alexandr Kandyba[13], Jonathan Brecko[3, 14], Martine Van den Broeck[15], Robert Losey[16], Jannikke Räikkönen[17], Mikhail Sablin[18], Julia Stagegaard[19], Shyam Gopalakrishnan[2,7], Sergey Fedorov[20], Mikkel-Holger S. Sinding[21], M. Thomas P. Gilbert[2,7,22], Nathan Wales[1]

1. Department of Archaeology, University of York, YO10 5NG York, UK
2. GLOBE Institute, University of Copenhagen, 1350 Copenhagen, Denmark
3. Royal Belgian Institute of Natural Sciences, 1000 Brussel, Belgium
4. Senckenberg Centre for Human Evolution and Palaeoenvironment (S-HEP), University of Tubingen, 72074 Tübingen, Germany
5. Department of Geosciences, Biogeology, University of Tübingen, 72076 Tübingen, Germany
6. Max Planck Institute of Geoanthropology, 07745 Jena, Germany
7. Centre for Evolutionary Hologenomics, University of Copenhagen, 1353 Copenhagen, Denmark
8. Centre for Palaeogenetics, Stockholm University, 106 91 Stockholm, Sweden
9. Department of Geological Sciences, Stockholm University, 114 18 Stockholm, Sweden
10. Cardiff School of Biosciences, Sir Martin Evans Building, Cardiff University, Museum Avenue, Cardiff CF10 3AX, UK
11. School of Biological and Behavioural Sciences, Queen Mary University of London, E1 4NS London, UK
12. Department of Bioinformatics and Genetics, Swedish Museum of Natural History, 104 05 Stockholm, Sweden

13. Institute of Archaeology and Ethnography SB RAS, Novosibirsk, 630090, Russia
14. Royal Museum for Central Africa, B-3080 Tervuren, Belgium
15. Faculty of Veterinary Medicine, Ghent University, 9820 Merelbeke, Belgium
16. Department of Anthropology, University of Alberta, Edmonton, AB T6G 2H4, Canada
17. Department of Environmental Monitoring and Research, Swedish Museum of Natural History, 104 05 Stockholm, Sweden
18. Zoological Institute of the Russian Academy of Sciences, 199034 St. Petersburg, Russia
19. Ree Park Safari, 8400 Ebeltoft, Denmark
20. Mammoth Museum of North-Eastern Federal University, 677000 Yakutsk, Russia
21. Department of Biology, University of Copenhagen, 2200 Copenhagen N, Denmark
22. NTNU University Museum, Norwegian University of Science and Technology, 7491 Trondheim, Norway

Corresponding Author:

Nathan Wales, Department of Archaeology, University of York, Environment Building, Wentworth Way, Heslington, York YO10 5NG, UK. Email: nathan.wales@york.ac.uk. +44 1904 328868

ABSTRACT

Distinguishing early domesticates from their wild progenitors presents a significant obstacle for understanding human-mediated impacts in the past. The origins of dogs is particularly controversial, as potential early dog remains often lack corroborating evidence that can provide secure links between proposed dog remains and human activity. The Tumat Puppies, two permafrost-preserved Late Pleistocene canids, have been hypothesised to have been littermates and early domesticates due to a physical association with putatively butchered mammoth bones. Through a combination of osteometry, stable isotope analysis, plant macrofossils analysis, and genomic and metagenomic analyses, this study exploits the unique properties of the naturally mummified Tumat Puppies to examine their familial relationship and to determine whether dietary information links them to human activities. The multifaceted analysis reveals the 14,965–14,046 cal yr BP Tumat Puppies were littermates who inhabited a dry and relatively mild environment with heterogeneous vegetation and consumed a diverse diet, including woolly rhinoceros in their final days. However, as there is no evidence of mammoth consumption, these data do not establish a link between the canids and ancient humans.

KEYWORDS

Osteometry, stable isotope analysis, macrofossils, metagenomics, ancient DNA, palaeogenomics, canids, dog domestication

INTRODUCTION

The dog is widely regarded as the first domesticated animal in human history, and its incorporation into human society has had profound impacts on human cultural adaptations (Morey, 2010; Losey et al., 2018). Despite decades of research, identifying the origin of dogs has been elusive (Benecke, 1987; Germonpré et al., 2009; Drake et al., 2015; Perri, 2016; Botigué et al., 2017; Thalmann and Perri, 2019), although recent findings suggests dogs may have been independently domesticated in more than one geographical region (Frantz et al., 2016; Bergström et al., 2022). The process of dog domestication has likewise been contentious, with one hypothesis arguing that humans actively captured and hand-raised wolves, with these socialized wolves becoming reproductively isolated from wild populations, ultimately giving rise to early dogs (Serpell, 1989, 2021; Müller, 2005; Germonpré et al., 2018, 2021; Mech and Janssens, 2022; Brumm et al., 2023). In contrast, a second hypothesis proposes a commensal pathway, in which wolves adapted to anthropogenic environments (Coppinger and Coppinger, 2001; Zeder, 2012; Larson and Fuller, 2014; Morey and Jeger, 2015). In this scenario, wolves initially scavenged around human settlements, gradually adapting to this new ecological niche. Over time, mutual habituation likely developed between the two species, eventually leading to a two-way partnership between wolves and humans (Zeder, 2012, 2015). To help resolve these hypotheses, unambiguous identification of early dogs in the archaeological record is needed. Recognition of early dog skeletal remains is often dependent on associated archaeological evidence that can provide direct connections to human activity. One example that provides such a link between dog skeletal remains and human activity is the 14,200-year-old Bonn-Oberkassel specimen, wherein a canid was interred alongside two adult humans (Janssens et al., 2018). Unfortunately, such examples, particularly from the Late Pleistocene, are very rare and often challenging to interpret. As a result, skeletal remains of several proposed early dogs are highly contested, and some have been revealed to belong to lineages of Pleistocene wolves that were separate from those that led to modern dogs (Ramos-Madrigal et al., 2021). When

such canid specimens are recovered from Late Pleistocene contexts, they warrant detailed, extensive investigations to clarify any potential connection to the history of dog domestication.

The so-called "Tumat Puppies" (Fig. 1) were discovered at a location in northern Siberia that has since been named the Syalakh site (Fig. 2). Tumat-1 (14,965–14,314 cal yr BP, Fig. 3, Supplementary Table 1 (Fedorov et al., 2014)) was discovered by mammoth ivory hunters from the village of Tumat in 2011 (Fedorov et al., 2014), while Tumat-2 (14,309–14,046 cal yr BP, Fig. 3, Supplementary Table 1 (Mak et al., 2017)) was uncovered during an excavation of the site in 2015 (Supplementary Figures 1–2). As originally described by Kandyba et al. (2015), the present day Syalakh site is situated on the eastern shore of an oxbow lake near the Syalakh River in the Sakha Republic (Yakutia), Russia, (Fig. 4.A). The site consists of a terrace that is eroding due to seasonal freezing and thawing cycles. Behind the solifluction apron, excavators identified five stratigraphic layers (Fig. 4.B), with the remains of the naturally mummified Tumat Puppies located between layers 2 and 3 in association with mammoth postcranial bones and a broken mammoth skull (Fedorov et al., 2014). Evidence of burning and human processing of the mammoth bones (Supplementary Figure 3) suggest that the Syalakh site may have been a mammoth butchering site.

Based on the proximity to putatively anthropogenic ecofacts, Fedorov et al. (2014) hypothesised the Tumat Puppies are early dogs. The association with the potential mammoth butchering site, if confirmed, could provide a compelling link to human activity, potentially leading to hypotheses that the Tumat Puppies were local domesticates, tamed wolves, or habituated scavengers. Although they were contemporaneous with the earliest confirmed Western European dogs (Janssens et al., 2018), Ramos-Madrigal et al.'s (2021) whole-genome analysis of Tumat-2 showed that this individual was not directly related to modern dogs. However, this genetic evidence could still be compatible with a scenario where the Tumat Puppies were part of a local domesticated lineage that went extinct without contributing to modern dog genetic history, or their pack could have been scavenging in

areas of human activity. Although Bergström et al. (2022) found a three base pair K^B deletion in Tumat-2, a genotype that gives rise to black fur and is believed to have introgressed from dogs into wolves, the unresolved status of the Tumat Puppies makes it difficult to assess whether the deletion evolved before or after canid domestication.

The exceptional preservation of the Tumat Puppies provides an opportunity to investigate their suggested association with the mammoth remains at the site through dietary reconstruction based on their hard and soft tissues and gastrointestinal (GI) content. A further hypothesis, based on the proximity of the two individuals as well as their visual similarities, suggests that the Tumat Puppies were siblings from the same litter. Through the combination of osteometry, stable isotope analysis, plant macrofossils, metagenomic analysis of the GI content, and genomic kinship analysis, this study evaluates the two hypotheses and obtains novel insight into the life and death of these two Pleistocene canids.

METHODS

In 2014, 2016 and 2018, subsamples were provided by SF and distributed to the individual researchers and institutes involved in this study for the purpose of the analyses summarised below. Detailed descriptions of all methods are available in the Supplementary Information (SI).

Radiocarbon dating

To evaluate whether putatively butchered mammoth bones from the Syalakh site are contemporaneous with the Tumat Puppies, a fragment of mammoth metacarpal was dated using accelerator mass spectrometry (AMS) at the Cenozoic Geochronology Center, Russia. The radiocarbon age of the mammoth and three published dates for the canids (Fedorov et al., 2014;

Mak et al., 2017; Lord et al., 2020) were calibrated with OxCal 4.4.4 (Ramsey, 2009) using the IntCal20 Northern Hemisphere radiocarbon age calibration curve (Reimer et al., 2020) (Supplementary Table 1). The uncertainty of the calibrated dates is reported using a 95.4% confidence interval (i.e., 2σ).

Description and osteometry

Briefly, the full bodies, limbs, and fur of both individuals (Fig. 1, Supplementary Figures 4–9) were measured and recorded. A full dissection was carried out on Tumat-1, and the stomach (Supplementary Figure 10) was found to contain identifiable feathers (e.g. subsample T1:S4, Supplementary Figure 11), as well as a piece of skin with hair still attached (subsample T1:S5, Supplementary Figure 12). Tumat-2 was not fully dissected but remained in a semi-frozen state. During the limited dissection of Tumat-2, the stomach was cut open (Supplementary Figure 13) allowing subsampling from different sections of the stomach, and an additional sample was taken from the rectum.

The crown length (CL) of the upper dP2 and dP3, and the lower dp2 and dp3 were measured with callipers. Computed tomography (CT) scans were used to calculate the length of the skull (Fig. 5.A), the length of the mandibula, the CL of the lower dp4 and of the germ of the lower carnassial (m1). The incompletely calcified crowns of the germs of the lower carnassials were reconstructed with Dragonfly 3.5 (Object Research Systems (ORS) Inc., 2018) in order to verify which cusps were present (Fig. 5.B). In dogs, antero-external cusps always develop first (Tims, 1896). The CL of the lower molars were calculated based on the models as though the complete mesiodistal CL in these teeth had been reached, even without the full development of the enamel. In completely developed dog molars, the maximum thickness of tooth enamel is about 1 mm (Crossley, 1995). The total CL of the lower first molar was estimated by adding 2✕1 mm to the calculated CL of the germs of the Tumat Puppies.

These measurements were compared with reference groups consisting of recent and ancient pups and adults of both wolves and dogs (Supplementary Tables 2–4). Age at death was determined by comparing the dentition of the Tumat Puppies with known deciduous and permanent dentition eruption sequences for several recent dog breeds and wolves. For Tumat-1, the age at death was also assessed based on fur development, where the length of the fur was measured in order to detect adult guard hair.

Stable isotope analysis

Elemental analysis (C, N, S) and isotopic analysis (δ^{13}C, δ^{15}N, δ^{34}S) were performed on bone, hair and tissue samples collected from both Tumat Puppies (Supplementary Tables 5–8). For bone collagen, the reliability of the δ^{13}C and δ^{15}N values can be established by measuring collagen chemical composition, with atomic C:N ranging from 2.9–3.6 (DeNiro, 1985) and the percentage of C and N above 8% and 3%, respectively (Ambrose, 1990). δ^{34}S values were retained from samples whose atomic C:S and N:S fit into the range of 300–900 and 100–300, respectively (Nehlich and Richards, 2009), and whose percentage of S ranged between 0.13% and 0.27%, determined through the results of modern mammalian collagen (cattle, elk and camel) measured in the same sets. In contrast to what is known about bone collagen, there are few, if any, widely accepted criteria for the quality control of skin, ligament, muscle, hair, and feather. However, as skin, ligament, and muscle are composed primarily of type I collagen, similar to bone, the same range for C:N, C:S and N:S ratios can arguably be applied for these tissues (e.g. Lamb, 2016). Limited information is available for isotopic values in hair and feathers, but the keratin protein that makes up these tissues contains a high abundance of cysteine leading to a likely increase in S content. An estimated C:N range of 3.0–4.0 is expected in hair according to published data (Kuitems et al., 2015; Szpak and Valenzuela, 2020) and internal analyses performed at the Tübingen laboratory, while a C:N range of 3.6–4.0 is anticipated for feather (Linglin et al., 2020). Further research is required to refine the quality criteria of S content

in hair and feathers, but until such a time, published data (Touzeau et al., 2014; Linglin et al., 2020; Lee et al., 2021) and internal analyses at the Tübingen laboratory suggest a range of 2.3–5.0% in S content is appropriate. Maternal prey choice was reconstructed by adjusting the tissue (i.e., hair) that provided the lowest δ^{15}N value to equivalent bone collagen values using the isotopic spacing between hair and collagen measured on the remains of a Palaeolithic cave lion (*Panthera spelaea*) from the Chukchi Peninsula (Kirillova et al., 2015). Measurements from subsamples TUM1-ST1 and TUM2-ST1h were adjusted to bone collagen values using the same calculations described above for the body hair. Measurements from the feathers in subsamples TUM1-ST3, TUM1-ST4 and TUM2-ST2 were adjusted to bone collagen values using the work of Hobson and Clark (1992). To complete the trophic web, published data were collected from large mammals from northeastern Siberia aged between ca. 16,400 and 12,000 ^{14}C yr BP (Supplementary Table 6).

Plant macrofossils

The stomach content samples were screened using an Olympus SZX 16 stereomicroscope, and plant remains were identified to the lowest possible taxonomic level using a reference collection at the Senckenberg Research Station of Quaternary Palaeontology and identification keys (Katz et al., 1965; Berggren, 1969, 1981; Anderberg, 1994). The taxa nomenclature follows the WFO Plant List (World Flora Online, 2024). The reconstruction of palaeo-vegetation followed the methodology of Kienast *et al.* (Kienast et al., 2005, 2008, 2011), and the identified vascular plant taxa were assigned to plant communities based on their ecological preferences and present day occurrences (Hilbig, 1995; Reinecke and Troeva, 2017).

Ancient DNA preparation and sequencing

Pre-PCR laboratory work was carried out in dedicated ancient DNA laboratory facilities in Copenhagen and Stockholm. Genomic DNA was extracted from seven GI samples from both Tumat-1 and Tumat-2 (Supplementary Table 9) following established methods for ancient DNA (Dabney et al., 2013; Allentoft et al., 2015; Rohland et al., 2018). Raw DNA was converted to double-stranded Illumina libraries, using either a seminal protocol used by many ancient DNA researchers (Meyer and Kircher, 2010) or the Blunt End Single Tube (BEST) protocol (Carøe et al., 2018) to reduce the number of purification steps and increase library complexity. Indexing PCR was carried out using unique dual indexes to improve the accuracy of multiplex sequencing (Kircher et al., 2012). Libraries were then sequenced across one lane of Illumina HiSeq 4000 in 80bp single-read mode.

DNA data processing

The raw DNA sequencing data was processed in a series of steps to remove contamination and ensure robust analyses were performed on authentic ancient DNA. First, the Illumina adapters used in sequencing were removed using AdapterRemoval/v2.3.1 (Schubert et al., 2016) and the quality of the resultant trimmed reads was assessed with FastQC/v0.11.8a (Andrews, 2010). Trimmed reads for all samples were then processed with PRINSEQ/v0.20.4 to filter uninformative low complexity sequences using the DUST algorithm (Schmieder and Edwards, 2011). To remove potential contaminant human DNA, reads were mapped against the human reference genome, hg38, using BWA/v0.7.17 (Li and Durbin, 2009) with the seed (the length of the initial sequence used for alignment) disabled to improve read mapping for ancient DNA (Schubert et al., 2012). Reads that did not map to the human genome were retained for further processing, using Samtools/v1.9 to select unmapped reads (Li et al., 2009) and bedtools/v2.26.0 BamToFastq to convert to fastq format (Quinlan, 2014). The non-human reads were then mapped to the wolf genome (Gopalakrishnan et al., 2017) using the previously described mapping strategy (Supplementary Table 10). PCR duplicates were removed using Picard/v2.6.0 (Broad Institute, 2019) and downstream analyses were limited to

reads with a mapping quality ≥30 indicating few, if any, errors. Four methods were used to explore the authenticity of the aligned reads: DNA fragment length, ancient DNA damage signatures at the ends of the reads using mapDamage 2.0 (Jónsson et al., 2013), read distribution across a genome of interest (Key et al., 2017), and edit distance (Jensen et al., 2019).

Kinship analysis

To analyse the relatedness of the Tumat Puppies, the reads that aligned to the wolf reference genome were merged with previously published genome-wide sequencing data from Tumat-1 and Tumat-2 (Mak et al., 2017; Bergström et al., 2022). Two approaches were used to evaluate kinship, one based on pseudo-haploid data using READ (Monroy Kuhn et al., 2018), the other a genotype likelihood method using NGSrelate/v20200904 (Hanghøj et al., 2019) with the R_0/R_1 and KING-robust estimators described in Waples et al. (2019). The expected values for the kinship estimators vary depending on the demographic history of the population, but such information is unavailable for the Tumat Puppies. Instead, a reference panel of unrelated and related canids, comprising genomic data from 5 Pleistocene wolves, 26 Eurasian grey wolves, 21 American grey wolves, and 11 Greenland village dogs (Supplementary Table 11) was compiled and used as a comparative dataset to enable the kinship analyses and interpret the results of the Tumat Puppies. The Greenland village dogs were included as an example of a population with a small population size and a high level of inbreeding.

Metagenomic analysis of GI content

The sequencing reads that did not align to the human and wolf reference genomes were aligned to all available mitochondrial genomes (downloaded from NCBI on 14/05-2020) using MALT/v.0.4.1 (Vågene et al., 2018) and a Last Common Ancestor (LCA) analysis was performed in MEGAN/v6.19.4 (Huson et al., 2016). All species with a substantial number of matching reads (≥ 500) were considered

to be “candidate species” and were subjected to further analysis to evaluate whether they were likely authentic. Specifically, the trimmed, non-human and non-wolf sequencing reads were mapped to the mitochondrial genomes of each candidate species, with a subsequent assessment of authenticity as described for the wolf DNA.

RESULTS

Chronology

The mammoth bone from the Syalakh site yielded an age of 14,308–13,480 cal yr BP (Fig. 3, Supplementary Table 1). As other analyses indicate Tumat-1 and Tumat-2 must be contemporaneous with each other (see kinship results), OxCal’s R_Combine function was used to combine three dates associated with the canids (14,965–14,314, 14,309–14,046 and 14,823–14,171 cal yr BP) in an attempt to refine the chronology. This combination of dates yielded a posterior distribution of 14,799–14,204 cal yr BP, which overlaps with the mammoth and could be compatible with the canids living when the mammoth butchering site was in use. However, this posterior distribution should be considered unreliable, as a χ^2-test implemented in OxCal fails at the 5% level, signifying the three dates from the Tumat Puppies are in poor agreement. The lack of fit of the three dates may be due to contamination of recent carbon in a sample or another unrecognised issue, but ultimately this inconsistency limits the chronological resolution. Without a clear justification to favour one set of AMS results, the Tumat Puppies can conservatively be considered to date within the full range of the calibrated dates (i.e., 14,965–14,046 cal yr BP), and no conclusions can be drawn from the dating on whether the canids may have been contemporaneous with the mammoth.

Description and osteometry

Physical description

Both of the Tumat Puppies were female based on their external genitalia. Their bodies were mostly intact (Fig. 1, Supplementary Figure 4–9), and measured 545 mm and 488 mm in length for Tumat-1 and Tumat-2 respectively, with tail lengths of 145 mm and 152 mm each. The ears and paws of both individuals were undamaged, and fur was preserved on both bodies. The fur was a monotone dark brown with no colour phases except on the palms and plantar parts of the paws, where pale hairs were present (Supplementary Figure 4, Supplementary Figure 7). The fur was relatively short and downy, and long guard hairs were absent. According to Kennedy (1982), adult guard hairs of wolves are 100–145 mm long on the back and 24–96 mm long on the belly. Detailed descriptions of the two specimens along with further analysis of Tumat-1's fur are available in the SI.

Osteometry

The skull of Tumat-1 had a total length of 127.1 mm, while the skull of Tumat-2 was 128.5 mm (Fig. 5.A, models are available, see Data Availability). The milk dentition of both Tumat Puppies was erupted and at full stature, and the lower first molars were in the intra-mandibular phases of formation (Supplementary Figure 5, Supplementary Figure 8). No permanent teeth were visible, and the first lower premolar in both specimens had yet to reach the alveolar ridge.

The CL of the deciduous teeth from both Tumat Puppies were compared with those from milk dentition of recent dogs and wolves (Supplementary Table 3). Although there was a small overlap between the observed ranges (OR) of all the milk teeth (except dp4) in dogs and wolves in the reference datasets, the means of the CL of the milk teeth of dogs were significantly smaller than those of wolves (Supplementary Table 3). In both Tumat Puppies, all measured deciduous teeth were larger than the lengths observed in the dog reference group, and within or larger than the recent

wolves reference group (Supplementary Table 3). The exception is dp2, which falls within the OR of the recent dog references but is smaller than that of the wolf reference group.

It was not possible to estimate the adult CL of the first lower molars (m1) of Tumat-1 because the germs did not reach their completed lengths. In Tumat-2, the crowns were complete, and the length of the full-grown left molar was estimated to 26.73 mm, while the right was estimated to 25.15 mm. As such, the length of the left lower molar fell within the ranges of Palaeolithic dogs and recent northern wolves, while the right lower molar fell in the OR of the Mesolithic Zhokhov dogs (Supplementary Table 4). Further details on the osteology and specific measurements are available in the SI.

Age at death

Mech (1970) observed that adult hairs appeared on the face of captive wolf pups at an age of 9 weeks and on the entire body at an age of 10 weeks. The absence of long, adult guard hairs on the face and body of the Tumat Puppies therefore suggested that they were younger than nine weeks at death. The completed eruption and full crown stature, the absence of shedding of the deciduous teeth, and the presence of an incompletely calcified crown of the lower carnassial further indicated that they were between seven and ten weeks of age at the time of death (Arnall, 1960; Shabestari et al., 1967; Esaka, 1982; Van den Broeck, 2022; Van den Broeck et al., 2022). In combination, this provided an estimate that both specimens were at least seven, but less than nine weeks old when they died.

Stable isotope analysis

The $\delta^{13}C$ values of the bone collagen, hair and tissue samples from Tumat-1 varied with less than 1‰ (Supplementary Table 7), which is consistent with intra-tissue isotopic variability. The $\delta^{15}N$ values (Supplementary Table 7) of the Tumat-1 bone collagen, ligament and hair samples were identical (+8.0‰), while the skin sample produced the highest value (+9.4‰). The higher $\delta^{15}N$ value obtained from skin provides the most recent isotopic information and likely reflects the ongoing consumption of mother's milk, which mimics the $\delta^{15}N$ enrichment observed in predators (e.g. Jenkins et al., 2001). For Tumat-2, the $\delta^{13}C$ values obtained from hair and muscle samples were 1–3‰ lower than those measured in the rib and scapula collagen of the same individual (Supplementary Table 7), a phenomenon that is not uncommon in mammals (e.g. Fox-Dobbs et al., 2007; Caut et al., 2009). Although the $\delta^{15}N$ values between the Tumat-2 tissues were comparable (Supplementary Table 7), the relatively high $\delta^{15}N$ value in the muscle (+9.1‰) is likely linked to the consumption of mother's milk, as with the skin sample from Tumat-1. The $\delta^{15}N$ enrichment due to suckling may also account for the slightly higher $\delta^{15}N$ values in rib collagen (+8.6‰) compared with scapula collagen (+8.3‰), resulting from potential higher collagen turnover in ribs. Although the most recently formed hair follicles also preserve the most recent isotopic values (e.g. Caut et al., 2009), the $\delta^{15}N$ values from the hair samples of both individuals did not reflect those obtained from the soft tissues, suggesting that the youngest part of the hair was not submitted for analysis.

Feathers from the stomach content of Tumat-1 showed relatively low $\delta^{13}C$ and high $\delta^{15}N$ values (Fig. 6, Supplementary Table 7) consistent with a freshwater ecosystem (e.g. Symes and Woodborne, 2010). The hair and skin samples from the same stomach content showed very different $\delta^{13}C$ and $\delta^{15}N$ values that suggests they come from a different individual or possibly another species (Fig. 6, Supplementary Table 7).

The $\delta^{34}S$ values measured on bone collagen, ligament, hair and skin from Tumat-1 and bone collagen and hair from Tumat-2 varied from +3.0 to +4.0‰ (Supplementary Table 8), illustrating a relative

homogeneity between the different tissues. Fractionation linked to trophic position is not expected in $\delta^{34}S$, leading to a relatively low intraindividual variability (Richards et al., 2003; Tanz and Schmidt, 2010). The $\delta^{34}S$ values observed in the Tumat Puppies are consistent with the local baseline of bioavailable sulphur in northeastern Siberia at the time, based on measurements from post-Last Glacial Maximum (LGM) mammoth remains from the Bykovsky Peninsula (Arppe et al., 2019).

Maternal prey choice

The measured $\delta^{13}C$ and $\delta^{15}N$ values of the Tumat Puppies and the reconstructed values of their mother are comparable to those of the Ulakhan Sular canid (Fig. 6, Supplementary Table 7), another post-LGM specimen geographically and morphometrically similar to the Tumat Puppies. The $\delta^{13}C$ and $\delta^{15}N$ values of the Berelekh mammoth remains are inconsistent with mammoth having constituted a significant proportion of the diet of the Tumat Puppies and their mother, due to lack of trophic enrichment in the canids compared to the mammoth. A large contribution from freshwater and marine ecosystems is also excluded. Instead, terrestrial ungulates, such as horse in combination with reindeer and possibly large bovids, likely comprised the majority of their diet (Supplementary Table 7).

Plant macrofossils

During the dissection, the stomach contents of Tumat-1 and Tumat-2 were visually similar, consisting of a light grey mass. Only Tumat-1 was fully thawed while Tumat-2 was not. As a result, identification of plant macrofossils was only carried out for Tumat-1. The most abundant remains were stems and leaves of grasses (Poaceae). A detailed inspection of the cellular structure of the plant suggests they belong to *Calamagrostis* sp. Several florets and achenes found within the stomach also belong to graminoids: *Hordeum jubatum* and *Carex* sect. Phacocystis cf. *minuta* (Fig. 7). Numerous twigs, two

buds and two almost complete leaves were identified as *Salix* sp. Complete shallowly lobed leaves belonging to *Dryas octopetala* were also observed. The only detected seeds were from *Pedicularis* cf. *labradorica* and *Poa* cf. *arctica*. Several moss species were observed within the sample. Invertebrate chitin remains were not abundant in the sample. Three complete elytra found in the stomach of Tumat-1 are identified as a dung-beetle *Aphodius* sp.

Kinship analysis

DNA sequenced from seven GI samples of each Tumat Puppy contained 0.1–18.3% canid DNA (Supplementary Table 10), with C-to-T misincorporations varying between 4.5–13.8% in the first position, consistent with damaged DNA molecules. The total coverage on the wolf reference genome was low—0.005 and 0.150× depth of coverage for Tumat-1 and Tumat-2, respectively—but in conjunction with published data from a tooth of Tumat-1 (Bergström et al., 2022) and soft tissues of Tumat-2 (Mak et al., 2017), the genome-wide data (Tumat-1=0.46× and Tumat-2=5.77×) enabled a kinship analysis.

Using READ (Monroy Kuhn et al., 2018), *P*0 between pairs of individuals in the reference wolf and dog populations was calculated and compared to the expected distribution of *P*0 of unrelated individuals. The results show that the distribution of *P*0 among Pleistocene wolves is close to that observed in modern grey wolves, thus these values can be used to identify relationships in Pleistocene canid populations. The *P*0 obtained for the Tumat Puppies falls outside the distribution of unrelated individuals and is similar to that obtained from three pairs of grey wolves with a full-sibling relationship (Fig. 8.A).

Using NGSrelate (Hanghøj et al., 2019), R_0/R_1 and KING-robust kinship coefficients between pairs of samples were estimated, with Tumat-1 and Tumat-2 falling within the expected values for half-sibling

relationships (Fig. 8.B). Given that the expected R_0/R_1 and kinship coefficients can vary in highly inbred populations, NGSrelate was also used to estimate inbreeding coefficients. NGSrelate determined that the Tumat Puppies (F_a=0.103613–0.120594) and most other Pleistocene wolves (F_a=0.1006–0.525134) had inbreeding coefficients comparable to that of modern Eurasian grey wolves (F_a=0.1006–0.6139).

The difference in kinship assignment between the READ and NGSrelate approaches is most likely due to the low depth of coverage of Tumat-1 genome, which particularly impacts NGSrelate (Marsh et al., 2023). It is further worth noting that kinship software packages are generally developed using human datasets, but demographic processes vary by species and allele frequencies from small reference panels may be inaccurate. Indeed, there are indications the allele frequencies of wolf populations may not be properly calibrated by NGSrelate, as the few individuals with known relationships do not exactly match theoretical expectations: the full-sibling relationships for U1, U2 and U3 individuals from Ree Park in Denmark have unexpectedly high values for R_1 and the parent-offspring relationships for individuals from Yellowstone National Park yield kinship coefficients that are similar to the values expected in unrelated pairs of individuals (Fig. 8.B). Nonetheless, both approaches indicate that the Tumat Puppies share at least a half-sibling relationship.

Metagenomic analysis of GI content

The MALT analysis of unmapped reads identified 37 taxa that had at least 500 reads mapped to their mitochondrial genomes. This candidate list of eukaryotes was subjected to a series of authenticity checks to differentiate between closely related species and evaluate which taxa may have been present in the GI system of the Tumat Puppies (Supplementary Table 12, Supplementary Figures 14–15). One of these species, wolf, was excluded from further analysis, as it had been confirmed previously and rather suggests the filtering of wolf DNA from the metagenomic dataset was not

entirely successful. The assignment of reads from each subsample revealed that the stomach content had a heterogeneous composition (Supplementary Table 12, Supplementary Table 13). Nine species of plants were detected in the T2:S5 and T2:CFM samples from Tumat-2, while another 20 plant species were found only in T2:CFM. As the MEGAN LCA analysis revealed that the majority of assigned plant mitochondrial reads clustered at higher taxonomic levels (Supplementary Figure 15), and given the complicated nature of plant mitochondrial phylogenies (Kowalczyk et al., 2021), an expanded authentication of the limited plant DNA data was not pursued.

In contrast to the limited plant DNA data, GI samples from both Tumat individuals yielded tens of thousands of DNA molecules matching the mitochondrial genome of woolly rhinoceros (*Coelodonta antiquitatis*) (Supplementary Table 13, Supplementary Figures 14–16). This is consistent with the previous recovery of a woolly rhinoceros mitochondrial genome from a single subsample of mummified tissue from the stomach of Tumat-1 (Lord et al., 2020). Two subsamples contained reads assigned to the mitochondrial genome of the extant Indian rhinoceros (*Rhinoceros unicornis*), but most failed to meet the minimum threshold for the edit distance, and all of the samples displayed an uneven read distribution despite high depth of coverage (Supplementary Table 13). In contrast, the reads that mapped to the woolly rhinoceros mitochondrial genome displayed a more even read distribution across the entire genome (Supplementary Table 13, Supplementary Figure 16), and edit distances were consistent with a good match between the aligned reads and the reference. Five of the seven subsamples from Tumat-1 and four of the seven subsamples from Tumat-2 met authentication criteria for woolly rhinoceros.

Sequencing reads from the T1:S2 and T1:S4 subsamples were identified as closely related to four potential avian species by the MALT analysis (Supplementary Table 12, Supplementary Figure 14): the white wagtail (*Motacilla alba*), the black-backed wagtail (*Motacilla alba lugens*), the grey wagtail (*Motacilla cinerea*) and the Hawaiian akikiki (*Oreomystis bairdi*). Although the late-Pleistocene range

of these species is not known, several species of wagtails, including the white wagtail and the grey wagtail, have breeding ranges that include Siberia today. While the majority of these species have yet to have their mitochondrial genomes sequenced, the western yellow wagtail (*Motacilla flava*), another summer inhabitant of Yakutia, was directly added to our candidate bird species panel using NCBI entry MW929090. Following the mapping and authentication steps, the akikiki could be rejected as the read distribution was highly uneven, with 52.3% of the mitochondrial genome without any coverage. In contrast, the mitochondrial genome of several wagtail species exhibited high and even coverage, as well as declining edit distances, which suggested a strong match between the reference genome and the data. The black-backed wagtail, the only non-resident of Siberia among the wagtail references, was a worse fit to the data, while the western yellow wagtail was found to have the highest mean depth of coverage (one sample reaching 152.0×), with 99.99% of positions represented. Although this indicates that the western yellow wagtail is the most likely candidate, the limited availability of wagtail reference genomes makes it difficult to conclusively identify which species of wagtail was eaten by Tumat-1.

DISCUSSION

The multifaceted analyses performed in this study provide detailed and unique insight into the lives and deaths of the two Late Pleistocene canid mummies known as the Tumat Puppies. Their state of preservation, with largely intact bodies complete with downy, dark brown fur, suggests that they were buried immediately after death. Based on their full stomachs, it is likely that they died rapidly, potentially due to a den collapse—similar to the scenario proposed for the Canadian Zhùr wolf pup mummy (Meachen et al., 2020)—or a landslide. Either event could account for the absence of traumatic injuries, however, it is interesting to note that this period was characterised by increased thermokarst activity (Walter et al., 2007), and rapid thawing of organic-rich permafrost could lead to landslides. Both Tumat Puppies were females in similar stages of development, and, based on the

length of the majority of their deciduous teeth, could be described as wolf-like in size. The presence of deciduous teeth, but the absence of adult guard hair, suggests that they perished between seven to nine weeks after parturition (Arnall, 1960; Shabestari et al., 1967; Mech, 1970; Esaka, 1982; Van den Broeck, 2022; Van den Broeck et al., 2022). Although wolf pups can already consume solids when a little older than three weeks (Mech, 2022), at seven to nine weeks, they start the transition from a milk-based diet to solids and begin eating regurgitated food provided by their mother and other pack members; they may even feed on small carcasses (Packard et al., 1992; Packard, 2003, 2019). The results of the stable isotope and metagenomic analyses on the Tumat Puppies are consistent with the dietary changes undergone by wolf pups during this stage of development. The multi-isotopic analyses did not indicate advanced weaning in the recently formed soft tissues, while the metagenomic analysis, which provided a snapshot of their last meal, demonstrated that the Tumat Puppies were both eating solids.

The Tumat Puppies were found in the same location, and based on their visual similarities, it has been hypothesised that they were littermates. The results of the analyses performed in this study support this hypothesis. The genetic kinship analyses indicated that the canids were either half- or full-siblings (Fig. 8), and a full-sibling relationship is arguably more likely given their comparable stage of development, the similarity of their diet, and what is known about modern wolf reproductive strategies. Both Tumat Puppies consumed woolly rhinoceros and although wagtail DNA was only detected in the stomach of Tumat-1, feathers were also recovered from Tumat-2 and included in the multi-isotopic analysis. In addition, no significant differences were found in the long-term dietary information recovered with stable isotope analysis. The inference that the Tumat Puppies were littermates is also consistent with present-day wolf pack composition. Wolf packs are territorial, multigenerational family groups. They can vary in size and complexity, depending on, for example, type and availability of prey. Pack complexity can also reflect pack size itself. Although large packs may include a second breeding pair, most often they are made up of one adult breeding pair and

their offspring (Mech, 1999; Tallian et al., 2023). Usually only one litter, comprising five to six pups on average, is born each season by the mother of the pack (Mech, 1999; Stahler et al., 2013). In the Siberian tundra today, wolf pups are born between the second half of May and the beginning of June (Heptner et al., 1998), which is consistent with the presence of wagtail in the stomach content, as wagtails in Northern Eurasia breed there in the warmer months before migrating south for the winter (Winkler et al., 2020).

The Tumat Puppies have previously been hypothesised to be early domestic dogs (Fedorov et al., 2014; Kandyba et al., 2015), as they were discovered at a potential butchering site containing burnt and cut mammoth bones (Supplementary Figure 3). Although this tangential link to humans sets them apart from other proposed Siberian early dog remains, corroborative evidence is needed to firmly establish a connection between the canids and human activities. Unfortunately, the currently available radiocarbon dates for the Tumat Puppies are not in close agreement and cannot be used to fully evaluate whether the butchered woolly mammoth remains were contemporaneous (Fig. 3). In contrast to the ambiguous chronology, the dietary analyses are more conclusive, with both the short- and long-term dietary reconstruction as performed in this study using metagenomics and stable isotope analyses suggesting that mammoth did not significantly contribute to the diet of the juveniles or their mother. Thus, there is no indication that the canids benefited from human activities, either by receiving food or by scavenging butchery sites. Rather than mammoth, the metagenomic analysis revealed that the last meal of the Tumat Puppies consisted of woolly rhinoceros and, in the case of Tumat-1, a wagtail. Observational studies of present-day wolves show that during the summer while some members of the pack are engaged in pup-rearing activities, wolf packs tend to subsist on smaller prey and often hunt ungulate neonates (Tallian et al., 2023). Consumption of megafauna such as woolly rhinoceros could therefore be construed as unusual based on recent wolf ecology. Notably, however, the piece of woolly rhinoceros skin recovered from Tumat-1's stomach (Supplementary Figure 12) was covered in blond fur. Although little is known

about the fur colour changes of the woolly rhinoceros during their lifespan, Chernova et al. (2016) found that hair from the calf known as “Sasha” was considerably lighter than that of adult members of the species. This could suggest that the meat in the Tumat Puppies’ stomachs came from a woolly rhinoceros calf, and so would coincide with present-day wolf hunting strategies that focus on juvenile prey (Tallian et al., 2023). In addition, the multi-isotopic dietary reconstruction predicted a generalist diet consisting primarily of terrestrial ungulates for the mother of the Tumat Puppies (Supplementary Table 7). Such a diet is consistent with the general trend observed in post-LGM large canids from Europe and eastern Beringia (Yeakel et al., 2013; Bocherens, 2015). Although the Tumat Puppies inhabited a diverse landscape that was also occupied by humans (e.g. Sikora et al., 2019), this study found no evidence that can conclusively link them to human activities. Arguments for early dog domestication require exceptional evidence, with a clear link between canid and human activities, but the results obtained here can be explained as Pleistocene wolf subsistence strategies and behaviour. This interpretation supports previous DNA evidence that places the Tumat Puppies on an ancient wolf lineage that did not contribute to the diversity of modern dogs (Ramos-Madrigal et al., 2021; Bergström et al., 2022). Thus, even if some canids from Late Pleistocene Siberia were supported by humans, the Tumat Puppies do not provide evidence for this process.

Beyond the question of domestication status, the results of the multifaceted analysis provide insights into the vegetation composition of the Tumat Puppies’ habitat. The radiocarbon dates of the two individuals fall on the transition from the Late-Weichselian stadial (ca. 15,000–12,500 ^{14}C yr BP as defined by Sher et al. (2005), which is approximately 18,000–14,500 cal yr BP). Prior to the transition, Sher et al. (2005) reconstruct a relatively mild but dry climate. This is followed by an increase in temperature and moisture that marked a major environmental change across the region and which led to widespread permafrost thaw (Sher et al., 2005; Walter et al., 2007). The mixture of plants, retrieved from the stomach content of Tumat-1, suggests a heterogeneous vegetation consistent with the banks of a river or oxbow lake shore, and it is not inconsistent with any point in this period

of climatic transition. The mixture of plants, retrieved from the stomach content of Tumat-1, suggests a heterogeneous vegetation structure characterised by both dry and moist environments consistent with the banks of a river or oxbow lake shore. Here, slope drainage would have made the slopes of the river terrace and oxbow lakes suitable for dry-tolerant vegetation such as *Dryas octopetala* (e.g. Vydrina et al., 1988; Kienast et al., 2008, 2011), while the floodplain would have provided conditions suitable for mesic vegetation, such as willow and the graminoids (grasses and sedges) that dominated the GI content. While wolves are primarily carnivores, they have been observed to feed their young with berries (Homkes et al., 2020), and consumption of grasses is a common behaviour of modern dogs (Bjone et al., 2007). It is possible, therefore, that the plant material may have been consumed for dietary reasons, but it could also have been ingested during play or exploration of the environment. The environmental conditions also align with present-day white and yellow wagtail breeding ranges, which are characterised by positive air temperatures and include tundra, floodplains, and the shores of water bodies (Ryzhanovskiy, 2018).

The success of this project highlights the potential of employing recent methodological advances to expand our knowledge of the Tumat Puppies and other organisms preserved in permafrost. One blossoming area of biomolecular research is palaeoproteomics (Warinner et al., 2022), through which mummified stomach tissue can be tested to infer more detailed dietary information (e.g. Grimm, 2021). For the Tumat Puppies, palaeoproteomics could allow detection of beta-lactoglobulin to determine if they had consumed milk shortly before dying. As advocated by Mann et al. (2023) for dental calculus, DNA enrichment methodologies would enable a deeper analysis of dietary DNA, thereby refining taxonomic identifications and potentially leading to population-level analyses of Pleistocene flora and fauna. To facilitate such an analysis, genomic data from extant wagtail species would be invaluable to understand past canid diets and Pleistocene ecology. Likewise, expansion of wild plant DNA reference panels beyond chloroplast sequences would facilitate taxonomic identifications and potentially offer gene-level analyses to explore adaptive responses across glacial

regimes. Finally, microbial DNA from mummified GI tracts could allow researchers to reconstruct ancestral microbiomes and elucidate millennia-scale evolution of the gut microbiome (e.g. Santiago-Rodriguez et al., 2015).

CONCLUSIONS

The Late Pleistocene Tumat Puppies have been an enigma in the search for the origins of dogs. While the canid pups fit the chronology of dog domestication and have previously been linked to human-modified woolly mammoth bones, this study suggests the most parsimonious interpretation is that they represent wolf littermates. This key inference is based on genetic data from the gut contents and stable isotopic signatures, neither of which indicate mammoth consumption by the pups nor their mother. As a possible link to humans was predicated on their proximity to butchered woolly mammoth bones, these findings support an alternate interpretation that the individuals belong to a wolf population that did not contribute to the lineages that led to modern dogs. In addition to shedding light on the domestication status of the Tumat Puppies, this multifaceted study leveraged the exceptionally well preserved remains to expand knowledge about the pups' kinship and diets, and the environment of Northern Siberia in the Late Pleistocene. Both pups were visually identified as female and genetic analysis revealed they are most likely littermates, which is consistent with sharing the same dietary components and being in a similar state of development, at seven to nine weeks of age. The gut contents reveal the pups were already eating solids, including woolly rhinoceros and, in the case of Tumat-1, a wagtail, but isotopic composition of their soft tissues suggested they continued to consume some milk. In concert with the DNA data, plant microfossils demonstrate the individuals inhabited a heterogeneous landscape that would have supported a range of flora and fauna. This work demonstrates the range of methods that can be applied to naturally mummified remains recovered from permafrost, as well as the potential of integrating disparate types of data to address controversial questions about Quaternary fauna.

ACKNOWLEDGEMENTS

A. K. W. Runge and J. Niemann were funded by the European Union's EU Framework Programme for Research and Innovation Horizon 2020 under Grant Agreement No. 676154. M. Sablin was supported by ZIN RAS (state assignment No. 122031100282-2). R. Losey was supported by SSHRC grant #G 435-2019-0706. Investigations by Alexander V. Kandyba were carried out as part of a government assignment to IAET SB RAS (Novosibirsk) No. FWZG-2024-0001. We thank Peter Tung and Valentina García-Huidobro (Senckenberg HEP, University of Tübingen) for their technical support in the analytical work for the isotope data. We express our appreciation to the Danish National High-throughput Sequencing Centre for assistance in generating the genomic sequencing data. The Viking cluster was used during this project, which is a high-performance computing facility provided by the University of York. We are grateful for computational support from the University of York, IT Services and the Research IT team. Map data copyrighted OpenStreetMap contributors and available from https://www.openstreetmap.org. We sincerely thank the reviewers for their insightful comments and constructive feedback, which greatly improved this manuscript. We also extend our gratitude to the editorial team and in particular, acknowledge Mary Edwards for highlighting a possible connection between the formation of the Syalakh site and thermokarst activity.

AUTHOR CONTRIBUTIONS

The project was conceived by MHSS, SF, MTPG, AKWR and NW. MG, MVdB, SF, JR, RL, and MS performed and interpreted the results of the descriptive and osteological analyses. HB and DGD performed and interpreted the results of the elemental and isotopic analyses. KB identified and interpreted the plant macrofossil analyses. AKWR, MHSS, and AL performed the genomic laboratory analyses of the GI content. JN, AKWR, NW and DS designed and performed the metagenomic

bioinformatic analyses, and interpreted the results. JR-M performed the kinship analysis and interpreted the results with input from SG. JS provided reference samples for the kinship analysis. AK interpreted the stratigraphy, and SF curated the archaeological material. AKWR and NW wrote the manuscript with input from MTPG, MG, DGD, HB, JR-M, KB and the other authors. All authors revised, edited and accepted the manuscript prior to publication.

COMPETING INTERESTS

The authors declare no competing interests.

DATA AVAILABILITY

The metagenomic dataset generated for this study is available in the NCBI BioProject PRJNA1093083.

3D models based on CT scans:

Tumat-1:

https://sketchfab.com/3d-models/tumat-cobaka-specimen-1-1cbd1e108be74c0dac02f93847b61c90

https://sketchfab.com/3d-models/tumat-cobaka-specimen-1-9a5d5e7649a3405aacc1739ad2bdeaf1

https://sketchfab.com/3d-models/tumat-cobaka-specimen-1-f2992ebed7e6491b8687f850289566c4

Tumat-2:

https://sketchfab.com/3d-models/tumat-cobaka-specimen-2-e15b8b70ac924b518900c1b9c16091ca

https://sketchfab.com/3d-models/tumat-cobaka-specimen-2-151e6d458e7446e6939c6b51f4e8e7e3

https://sketchfab.com/3d-models/tumat-cobaka-specimen-2-f9c845cfa256477fa089e318683a2f99

REFERENCES

Allentoft, M.E., Sikora, M., Sjögren, K.-G., Rasmussen, S., Rasmussen, M., Stenderup, J., Damgaard, P.B., Schroeder, H., Ahlström, T., Vinner, L., Malaspinas, A.-S., Margaryan, A., Higham, T., Chivall, D., Lynnerup, N., Harvig, L., Baron, J., Della Casa, P., Dąbrowski, P., Duffy, P.R., Ebel, A.V., Epimakhov, A., Frei, K., Furmanek, M., Gralak, T., Gromov, A., Gronkiewicz, S., Grupe, G., Hajdu, T., Jarysz, R., Khartanovich, V., Khokhlov, A., Kiss, V., Kolář, J., Kriiska, A., Lasak, I., Longhi, C., McGlynn, G., Merkevicius, A., Merkyte, I., Metspalu, M., Mkrtchyan, R., Moiseyev, V., Paja, L., Pálfi, G., Pokutta, D., Pospieszny, Ł., Price, T.D., Saag, L., Sablin, M., Shishlina, N., Smrčka, V., Soenov, V.I., Szeverényi, V., Tóth, G., Trifanova, S.V., Varul, L., Vicze, M., Yepiskoposyan, L., Zhitenev, V., Orlando, L., Sicheritz-Pontén, T., Brunak, S., Nielsen, R., Kristiansen, K., Willerslev, E., 2015. Population genomics of Bronze Age Eurasia. *Nature* 522, 167–172.

Ambrose, S.H., 1990. Preparation and characterization of bone and tooth collagen for isotopic analysis. *Journal of Archaeological Science* 17, 431–451.

Anderberg, A.-L., 1994. *Resedaceae-Umbelliferae. Atlas of Seeds and Small Fruits of Northwest-European Plant Species with Morphological Descriptions, 4*. Swedish Museum of Natural History, Stockholm, Stockholm.

Andrews, S., 2010. *FastQC: a quality control tool for high throughput sequence data*. Babraham Bioinformatics, Babraham Institute, Cambridge, United Kingdom.

Arnall, L., 1960. Some aspects of dental development in the dog-II. Eruption and extrusion. *Journal of Small Animal Practice* 1, 259–267.

Arppe, L., Karhu, J.A., Vartanyan, S., Drucker, D.G., Etu-Sihvola, H., Bocherens, H., 2019. Thriving or surviving? The isotopic record of the Wrangel Island woolly mammoth population. *Quaternary Science Reviews* 222, 105884.

Benecke, N., 1987. Studies on early dog remains from Northern Europe. *Journal of Archaeological Science* 14, 31–49.

Berggren, G., 1981. *Salicaceaee, Cruciferae. Atlas of Seeds and Small Fruits of Northwest-European Plant Species with Morphological Descriptions, 3*. Swedish Museum of Natural History, Stockholm, Stockholm.

Berggren, G., 1969. *Cyperaceae. Atlas of Seeds and Small Fruits of Northwest- European Plant Species with Morphological Descriptions, 2*. Swedish Natural Science Research Council, Stockholm, Stockholm.

Bergström, A., Stanton, D.W.G., Taron, U.H., Frantz, L., Sinding, M.-H.S., Ersmark, E., Pfrengle, S., Cassatt-Johnstone, M., Lebrasseur, O., Girdland-Flink, L., Fernandes, D.M., Ollivier, M., Speidel, L., Gopalakrishnan, S., Westbury, M.V., Ramos-Madrigal, J., Feuerborn, T.R., Reiter, E., Gretzinger, J., Münzel, S.C., Swali, P., Conard, N.J., Carøe, C., Haile, J., Linderholm, A., Androsov, S., Barnes, I., Baumann, C., Benecke, N., Bocherens, H., Brace, S., Carden, R.F., Drucker, D.G., Fedorov, S., Gasparik, M., Germonpré, M., Grigoriev, S., Groves, P., Hertwig, S.T., Ivanova, V.V., Janssens, L., Jennings, R.P., Kasparov, A.K., Kirillova, I.V., Kurmaniyazov, I., Kuzmin, Y.V., Kosintsev, P.A., Lázničková-Galetová, M., Leduc, C., Nikolskiy, P., Nussbaumer, M., O'Drisceoil, C., Orlando, L., Outram, A., Pavlova, E.Y., Perri, A.R., Pilot, M., Pitulko, V.V., Plotnikov, V.V., Protopopov, A.V., Rehazek, A., Sablin, M., Seguin-Orlando, A., Storå, J., Verjux, C., Zaibert, V.F., Zazula, G., Crombé, P., Hansen, A.J., Willerslev, E., Leonard, J.A., Götherström, A., Pinhasi, R., Schuenemann, V.J., Hofreiter, M., Gilbert, M.T.P., Shapiro, B., Larson, G., Krause, J., Dalén, L., Skoglund, P., 2022. Grey wolf genomic history reveals a dual ancestry of dogs. *Nature* 607, 313–320.

Bjone, S.J., Brown, W.Y., Price, I.R., 2007. Grass eating patterns in the domestic dog, *Canis familiaris*. *Recent Advances in Animal Nutrition in Australia* 16, 45–49.

Bocherens, H., 2015. Isotopic tracking of large carnivore palaeoecology in the mammoth steppe. *Quaternary Science Reviews* 117, 42–71.

Botigué, L.R., Song, S., Scheu, A., Gopalan, S., Pendleton, A.L., Oetjens, M., Taravella, A.M., Seregély,

T., Zeeb-Lanz, A., Arbogast, R.-M., Bobo, D., Daly, K., Unterländer, M., Burger, J., Kidd, J.M., Veeramah, K.R., 2017. Ancient European dog genomes reveal continuity since the Early Neolithic. *Nature Communications* 8, 16082.

Broad Institute, 2019. *Picard Toolkit GitHub Repository. http://broadinstitute.github.io/picard/*.

Brumm, A., Germonpré, M., Koungoulos, L., 2023. The human-initiated model of wolf domestication - An expansion based on human-dingo relations in Aboriginal Australia. *Frontiers in Psychology* 14, 1082338.

Carøe, C., Gopalakrishnan, S., Vinner, L., Mak, S.S.T., Sinding, M.H.S., Samaniego, J.A., Wales, N., Sicheritz-Pontén, T., Gilbert, M.T.P., 2018. Single-tube library preparation for degraded DNA. *Methods in Ecology and Evolution* 9, 410–419.

Caut, S., Angulo, E., Courchamp, F., 2009. Variation in discrimination factors (Δ^{15}N and Δ^{13}C): the effect of diet isotopic values and applications for diet reconstruction. *The Journal of Applied Ecology* 46, 443–453.

Chernova, O.F., Protopopov, A.V., Perfilova, T.V., Kirillova, I.V., Boeskorov, G.G., 2016. Hair microstructure of the first time found calf of woolly rhinoceros *Coelodonta antiquitatis*. *Doklady Biological Sciences* 471, 291–295.

Coppinger, R., Coppinger, L., 2001. *Dogs: A new understanding of canine origin, behavior, and evolution*. University of Chicago Press, Chicago.

Crossley, D.A., 1995. Tooth enamel thickness in the mature dentition of domestic dogs and cats--preliminary study. *Journal of Veterinary Dentistry* 12, 111–113.

Dabney, J., Knapp, M., Glocke, I., Gansauge, M.-T., Weihmann, A., Nickel, B., Valdiosera, C., García, N., Pääbo, S., Arsuaga, J.-L., Meyer, M., 2013. Complete mitochondrial genome sequence of a Middle Pleistocene cave bear reconstructed from ultrashort DNA fragments. *Proceedings of the National Academy of Sciences of the United States of America* 110, 15758–15763.

DeNiro, M.J., 1985. Postmortem preservation and alteration of in vivo bone collagen isotope ratios in relation to palaeodietary reconstruction. *Nature* 317, 806–809.

Drake, A.G., Coquerelle, M., Colombeau, G., 2015. 3D morphometric analysis of fossil canid skulls contradicts the suggested domestication of dogs during the late Paleolithic. *Scientific Reports* 5, 8299.

Esaka, S., 1982. Development of rotation of mandibular premolar tooth germs in the dog. *Acta Anatomica* 114, 211–227.

Fedorov, S., Garmaeva, D., Luginov, N., Grigoriev, S., Savvinov, G., Vasilev, S., Kirikov, K., Allentoft, M., Tikhonov, A., 2014. Tomographic study and 3D-reconstruction of mummified Pleistocene dog from North-Eastern Siberia. *Scientific Annals of the School of Geology, Aristotle University of Thessaloniki* 102, 53.

Fox-Dobbs, K., Bump, J.K., Peterson, R.O., Fox, D.L., Koch, P.L., 2007. Carnivore-specific stable isotope variables and variation in the foraging ecology of modern and ancient wolf populations: case studies from Isle Royale, Minnesota, and La Brea. *Canadian Journal of Zoology* 85, 458–471.

Frantz, L.A.F., Mullin, V.E., Pionnier-Capitan, M., Lebrasseur, O., Ollivier, M., Perri, A., Linderholm, A., Mattiangeli, V., Teasdale, M.D., Dimopoulos, E.A., Tresset, A., Duffraisse, M., McCormick, F., Bartosiewicz, L., Gál, E., Nyerges, É.A., Sablin, M.V., Bréhard, S., Mashkour, M., Bălăşescu, A., Gillet, B., Hughes, S., Chassaing, O., Hitte, C., Vigne, J.-D., Dobney, K., Hänni, C., Bradley, D.G., Larson, G., 2016. Genomic and archaeological evidence suggest a dual origin of domestic dogs. *Science* 352, 1228–1231.

Germonpré, M., Lázničková-Galetová, M., Sablin, M.V., Bocherens, H., 2018. Self-domestication or human control? The Upper Palaeolithic domestication of the wolf, in: Stépanoff, C., Vigne, J.-D. (Eds.), Hybrid Communities. Routledge, pp. 39–64.

Germonpré, M., Sablin, M.V., Stevens, R.E., Hedges, R.E.M., Hofreiter, M., Stiller, M., Després, V.R., 2009. Fossil dogs and wolves from Palaeolithic sites in Belgium, the Ukraine and Russia: osteometry, ancient DNA and stable isotopes. *Journal of Archaeological Science* 36, 473–490.

Germonpré, M., Van den Broeck, M., Lázničková-Galetová, M., Sablin, M.V., Bocherens, H., 2021.

Mothering the Orphaned Pup: The Beginning of a Domestication Process in the Upper Palaeolithic. *Human Ecology* 49, 677–689.
Gopalakrishnan, S., Samaniego Castruita, J.A., Sinding, M.-H.S., Kuderna, L.F.K., Räikkönen, J., Petersen, B., Sicheritz-Ponten, T., Larson, G., Orlando, L., Marques-Bonet, T., Hansen, A.J., Dalén, L., Gilbert, M.T.P., 2017. The wolf reference genome sequence (*Canis lupus lupus*) and its implications for *Canis* spp. population genomics. *BMC Genomics* 18, 495.
Grimm, R., 2021. How modern mass spectrometry can solve ancient questions: A multi-omics study of the stomach content of the oldest human ice mummy, the 5300-year-old Iceman or Oetzi. *Methods in Molecular Biology* 2261, 1–12.
Hanghøj, K., Moltke, I., Andersen, P.A., Manica, A., Korneliussen, T.S., 2019. Fast and accurate relatedness estimation from high-throughput sequencing data in the presence of inbreeding. *Gigascience* 8, giz034.
Heptner, V.G., Naumov, N.P., Yurgenson, P.B., Sludskii, A.A., Chirkova, A.F., & Bannikov, A.G., 1998. *Mammals of the Soviet Union. Volume II. Part la, Sirenia and Carnivora*. Washington DC: Smithsonian Institution Libraries and National Science Foundation.
Hilbig, W., 1995. *The Vegetation of Mongolia*. SPB Academic Publishing, The Hague, Netherlands.
Hobson, K.A., Clark, R.G., 1992. Assessing Avian Diets Using Stable Isotopes II: Factors Influencing Diet-Tissue Fractionation. *Condor* 94, 189–197.
Homkes, A.T., Gable, T.D., Windels, S.K., Bump, J.K., 2020. Berry important? Wolf provisions pups with berries in northern Minnesota. *Wildlife Society Bulletin* 44, 221–223.
Huson, D.H., Beier, S., Flade, I., Górska, A., El-Hadidi, M., Mitra, S., Ruscheweyh, H.-J., Tappu, R., 2016. MEGAN Community Edition - Interactive Exploration and Analysis of Large-Scale Microbiome Sequencing Data. *PLoS Computational Biology* 12, e1004957.
Janssens, L., Giemsch, L., Schmitz, R., Street, M., Van Dongen, S., Crombé, P., 2018. A new look at an old dog: Bonn-Oberkassel reconsidered. *Journal of Archaeological Science* 92, 126–138.
Jenkins, S.G., Partridge, S.T., Stephenson, T.R., Farley, S.D., Robbins, C.T., 2001. Nitrogen and carbon isotope fractionation between mothers, neonates, and nursing offspring. *Oecologia* 129, 336–341.
Jensen, T.Z.T., Niemann, J., Iversen, K.H., Fotakis, A.K., Gopalakrishnan, S., Vågene, Å.J., Pedersen, M.W., Sinding, M.-H.S., Ellegaard, M.R., Allentoft, M.E., Lanigan, L.T., Taurozzi, A.J., Nielsen, S.H., Dee, M.W., Mortensen, M.N., Christensen, M.C., Sørensen, S.A., Collins, M.J., Gilbert, M.T.P., Sikora, M., Rasmussen, S., Schroeder, H., 2019. A 5700 year-old human genome and oral microbiome from chewed birch pitch. *Nature Communications* 10, 5520.
Jónsson, H., Ginolhac, A., Schubert, M., Johnson, P.L.F., Orlando, L., 2013. mapDamage2.0: fast approximate Bayesian estimates of ancient DNA damage parameters. *Bioinformatics* 29, 1682–1684.
Kandyba, A.V., Fedorov, S.E., Dmitriev, A.I., Protodiakonov, K.I., 2015. A new late Neo-Pleistocene archaeological object Syalakh site in the Russian Arctic region (in Russian). *Problems of Archaeology, Ethnography, Anthropology of Siberia and Neighboring Territories* 21, 90–93.
Katz, N.Y., Katz, S.V., Kipiani, M.G., 1965. *Atlas and Keys of Fruits and Seeds Occurring in the Quaternary Deposits of The USSR*, Academy of sciences of the USSR. Izd. Nauka, Moscow.
Kennedy, A.J., 1982. Distinguishing characteristics of the hairs of wild and domestic canids from Alberta. *Canadian Journal of Zoology* 60, 536–541.
Key, F.M., Posth, C., Krause, J., Herbig, A., Bos, K.I., 2017. Mining Metagenomic Data Sets for Ancient DNA: Recommended Protocols for Authentication. *Trends in Genetics* 33, 508–520.
Kienast, F., Schirrmeister, L., Siegert, C., Tarasov, P., 2005. Palaeobotanical evidence for warm summers in the East Siberian Arctic during the last cold stage. *Quaternary Research* 63, 283–300.
Kienast, F., Tarasov, P., Schirrmeister, L., Grosse, G., Andreev, A.A., 2008. Continental climate in the East Siberian Arctic during the last interglacial: Implications from palaeobotanical records. *Global and Planetary Change* 60, 535–562.

Kienast, F., Wetterich, S., Kuzmina, S., Schirrmeister, L., Andreev, A.A., Tarasov, P., Nazarova, L., Kossler, A., Frolova, L., Kunitsky, V.V., 2011. Paleontological records indicate the occurrence of open woodlands in a dry inland climate at the present-day Arctic coast in western Beringia during the Last Interglacial. *Quaternary Science Reviews* 30, 2134–2159.

Kircher, M., Sawyer, S., Meyer, M., 2012. Double indexing overcomes inaccuracies in multiplex sequencing on the Illumina platform. *Nucleic Acids Research* 40, e3.

Kirillova, I.V., Tiunov, A.V., Levchenko, V.A., Chernova, O.F., Yudin, V.G., Bertuch, F., Shidlovskiy, F.K., 2015. On the discovery of a cave lion from the Malyi Anyui River (Chukotka, Russia). *Quaternary Science Reviews* 117, 135–151.

Kowalczyk, M., Staniszewski, A., Kamiñska, K., Domaradzki, P., Horecka, B., 2021. Advantages, Possibilities, and Limitations of Mitochondrial DNA Analysis in Molecular Identification. *Folia Biologica* 69, 101–111.

Kuitems, M., Van Kolfschoten, T., van der Plicht, J., 2015. Elevated $\delta^{15}N$ values in mammoths: a comparison with modern elephants. *Archaeological and Anthropological Sciences*.

Lamb, A.L., 2016. Stable isotope analysis of soft tissues from mummified human remains. *Environmental Archaeology*.

Larson, G., Fuller, D.Q., 2014. The Evolution of Animal Domestication. *Annual Review of Ecology, Evolution, and Systematics* 45, 115–136.

Lee, H.-S., Shim, J.-Y., Shin, W.-J., Choi, S.-H., Bong, Y.-S., Lee, K.-S., 2021. Dietary homogenization and spatial distributions of carbon, nitrogen, and sulfur isotope ratios in human hair in South Korea. *PLoS One* 16, e0256404.

Li, H., Durbin, R., 2009. Fast and accurate short read alignment with Burrows-Wheeler transform. *Bioinformatics* 25, 1754–1760.

Li, H., Handsaker, B., Wysoker, A., Fennell, T., Ruan, J., Homer, N., Marth, G., Abecasis, G., Durbin, R., 1000 Genome Project Data Processing Subgroup, 2009. The Sequence Alignment/Map format and SAMtools. *Bioinformatics* 25, 2078–2079.

Linglin, M., Amiot, R., Richardin, P., Porcier, S., 2020. Isotopic systematics point to wild origin of mummified birds in Ancient Egypt. *Scientific Reports*.

Lord, E., Dussex, N., Kierczak, M., Díez-Del-Molino, D., Ryder, O.A., Stanton, D.W.G., Gilbert, M.T.P., Sánchez-Barreiro, F., Zhang, G., Sinding, M.-H.S., Lorenzen, E.D., Willerslev, E., Protopopov, A., Shidlovskiy, F., Fedorov, S., Bocherens, H., Nathan, S.K.S.S., Goossens, B., van der Plicht, J., Chan, Y.L., Prost, S., Potapova, O., Kirillova, I., Lister, A.M., Heintzman, P.D., Kapp, J.D., Shapiro, B., Vartanyan, S., Götherström, A., Dalén, L., 2020. Pre-extinction Demographic Stability and Genomic Signatures of Adaptation in the Woolly Rhinoceros. *Current Biology* 30, 3871–3879.e7.

Losey, R.J., Wishart, R.P., Loovers, J.P.L., 2018. *Dogs in the North: Stories of Cooperation and Co-Domestication*. Routledge, Abingdon-on-Thames, UK.

Mak, S.S.T., Gopalakrishnan, S., Carøe, C., Geng, C., Liu, S., Sinding, M.-H.S., Kuderna, L.F.K., Zhang, W., Fu, S., Vieira, F.G., Germonpré, M., Bocherens, H., Fedorov, S., Petersen, B., Sicheritz-Pontén, T., Marques-Bonet, T., Zhang, G., Jiang, H., Gilbert, M.T.P., 2017. Comparative performance of the BGISEQ-500 vs Illumina HiSeq2500 sequencing platforms for palaeogenomic sequencing. *Gigascience* 6, 1–13.

Mann, A.E., Fellows Yates, J.A., Fagernäs, Z., Austin, R.M., Nelson, E.A., Hofman, C.A., 2023. Do I have something in my teeth? The trouble with genetic analyses of diet from archaeological dental calculus. *Quaternary International* 653-654, 33–46.

Marsh, W.A., Brace, S., Barnes, I., 2023. Inferring biological kinship in ancient datasets: comparing the response of ancient DNA-specific software packages to low coverage data. *BMC Genomics* 24, 111.

Meachen, J., Wooller, M.J., Barst, B.D., Funck, J., Crann, C., Heath, J., Cassatt-Johnstone, M., Shapiro, B., Hall, E., Hewitson, S., Zazula, G., 2020. A mummified Pleistocene gray wolf pup. *Current Biology* 30, R1467–R1468.

Mech, L.D., 2022. Newly Documented Behavior of Free-Ranging Arctic Wolf Pups. *Arctic* 75, 272–276.

Mech, L.D., 1999. Alpha status, dominance, and division of labor in wolf packs. *Canadian Journal of Zoology*.
Mech, L.D., 1970. *The wolf: the ecology and behavior of an endangered species*. Natural History Press, New York.
Mech, L.D., Janssens, L.A.A., 2022. An assessment of current wolf *Canis lupus* domestication hypotheses based on wolf ecology and behaviour. *Mammal Review* 52, 304–314.
Meyer, M., Kircher, M., 2010. Illumina sequencing library preparation for highly multiplexed target capture and sequencing. *Cold Spring Harbor Protocols* 2010, db.prot5448.
Monroy Kuhn, J.M., Jakobsson, M., Günther, T., 2018. Estimating genetic kin relationships in prehistoric populations. *PLoS One* 13, e0195491.
Morey, D., 2010. *Dogs: Domestication and the Development of a Social Bond*. Cambridge University Press, Cambridge, UK.
Morey, D.F., Jeger, R., 2015. Paleolithic dogs: Why sustained domestication then? *Journal of Archaeological Science: Reports* 3, 420–428.
Müller, W., 2005. The domestication of the wolf - the inevitable first?, in: Vigne, J.-D., Peters, J., Helmer, D. (Eds.), The First Steps of Animal Domestication, Proceedings of the 9th ICAZ Conference, Durham. Oxford: Oxbow Books, pp. 34–40.
Nehlich, O., Richards, M.P., 2009. Establishing collagen quality criteria for sulphur isotope analysis of archaeological bone collagen. *Archaeological and Anthropological Sciences* 1, 59–75.
Object Research Systems (ORS) Inc., 2018. *Dragonfly 3.5*.
OpenStreetMap contributors, 2017. OpenStreetMap. *https://www.openstreetmap.org*.
Packard, J.M., 2019. Wolves, in: Choe, J.C. (Ed.), Encyclopedia of Animal Behavior, Second Edition. Academic Press, Oxford, pp. 262–278.
Packard, J.M., 2003. Wolf behaviour : reproductive, social and intelligent, in: Mech, L.D., Boitani, L. (Eds.), Wolves: Behavior, Ecology, and Conservation. University of Chicago Press, Chicago, pp. 35–65.
Packard, J.M., Mech, L.D., Ream, R.R., 1992. Weaning in an arctic wolf pack: behavioral mechanisms. *Canadian Journal of Zoology* 70, 1269–1275.
Perri, A.R., 2016. A wolf in dog's clothing: Initial dog domestication and Pleistocene wolf variation. *Journal of Archaeological Science* 68, 1–4.
QGIS Development Team, 2023. QGIS Geographic Information System. QGIS Association.
Quinlan, A.R., 2014. BEDTools: The Swiss-Army Tool for Genome Feature Analysis. *Current Protocols in Bioinformatics* 47, 11.12.1–34.
Ramos-Madrigal, J., Sinding, M.-H.S., Carøe, C., Mak, S.S.T., Niemann, J., Samaniego Castruita, J.A., Fedorov, S., Kandyba, A., Germonpré, M., Bocherens, H., Feuerborn, T.R., Pitulko, V.V., Pavlova, E.Y., Nikolskiy, P.A., Kasparov, A.K., Ivanova, V.V., Larson, G., Frantz, L.A.F., Willerslev, E., Meldgaard, M., Petersen, B., Sicheritz-Ponten, T., Bachmann, L., Wiig, Ø., Hansen, A.J., Gilbert, M.T.P., Gopalakrishnan, S., 2021. Genomes of Pleistocene Siberian Wolves Uncover Multiple Extinct Wolf Lineages. *Current Biology* 31, 198–206.
Ramsey, C.B., 2009. Bayesian Analysis of Radiocarbon Dates. *Radiocarbon* 51, 337–360.
Reimer, P.J., Austin, W.E.N., Bard, E., Bayliss, A., Blackwell, P.G., Ramsey, C.B., Butzin, M., Cheng, H., Lawrence Edwards, R., Friedrich, M., Grootes, P.M., Guilderson, T.P., Hajdas, I., Heaton, T.J., Hogg, A.G., Hughen, K.A., Kromer, B., Manning, S.W., Muscheler, R., Palmer, J.G., Pearson, C., van der Plicht, J., Reimer, R.W., Richards, D.A., Marian Scott, E., Southon, J.R., Turney, C.S.M., Wacker, L., Adolphi, F., Büntgen, U., Capano, M., Fahrni, S.M., Fogtmann-Schulz, A., Friedrich, R., Köhler, P., Kudsk, S., Miyake, F., Olsen, J., Reinig, F., Sakamoto, M., Sookdeo, A., Talamo, S., 2020. The IntCal20 Northern Hemisphere Radiocarbon Age Calibration Curve (0–55 cal kBP). *Radiocarbon* 62, 725–757.
Reinecke, J., Troeva, E., 2017. Extrazonal steppes and other temperate grasslands of northern Siberia − Phytosociological classification and ecological characterization. *Phytocoenologia* 47, 167–196.
Richards, M.P., Fuller, B.T., Sponheimer, M., Robinson, T., Ayliffe, L., 2003. Sulphur isotopes in

palaeodietary studies: a review and results from a controlled feeding experiment. *International Journal of Osteoarchaeology* 13, 37–45.
Rohland, N., Glocke, I., Aximu-Petri, A., Meyer, M., 2018. Extraction of highly degraded DNA from ancient bones, teeth and sediments for high-throughput sequencing. *Nature Protocols* 13, 2447–2461.
Ryzhanovskiy, V.N., 2018. Annual Cycles of Wagtails (Passeriformes, Motacillidae) in Northwestern Siberia: Comparative Aspects. *Biology Bulletin* 45, 1055–1066.
Santiago-Rodriguez, T.M., Fornaciari, G., Luciani, S., Dowd, S.E., Toranzos, G.A., Marota, I., Cano, R.J., 2015. Gut Microbiome of an 11th Century A.D. Pre-Columbian Andean Mummy. *PLoS One* 10, e0138135.
Schmieder, R., Edwards, R., 2011. Quality control and preprocessing of metagenomic datasets. *Bioinformatics* 27, 863–864.
Schubert, M., Ginolhac, A., Lindgreen, S., Thompson, J.F., Al-Rasheid, K.A.S., Willerslev, E., Krogh, A., Orlando, L., 2012. Improving ancient DNA read mapping against modern reference genomes. *BMC Genomics* 13, 178.
Schubert, M., Lindgreen, S., Orlando, L., 2016. AdapterRemoval v2: rapid adapter trimming, identification, and read merging. *BMC Research Notes* 9, 88.
Serpell, J., 1989. Pet-keeping and animal domestication: a reappraisal, in: Clutton-Brock, J. (Ed.), The Walking Larder: Patterns of Domestication, Pastoralism, and Predation. London: Unwin Hyman, pp. 10–21.
Serpell, J.A., 2021. Commensalism or Cross-Species Adoption? A Critical Review of Theories of Wolf Domestication. *Frontiers in Veterinary Science* 8, 662370.
Shabestari, L., Taylor, G.N., Angus, W., 1967. Dental eruption pattern of the Beagle. *Journal of Dental Research* 46, 276–278.
Sher, A.V., Kuzmina, S.A., Kuznetsova, T.V., Sulerzhitsky, L.D., 2005. New insights into the Weichselian environment and climate of the East Siberian Arctic, derived from fossil insects, plants, and mammals. *Quaternary Science Reviews* 24, 533–569.
Sikora, M., Pitulko, V.V., Sousa, V.C., Allentoft, M.E., Vinner, L., Rasmussen, S., Margaryan, A., de Barros Damgaard, P., de la Fuente, C., Renaud, G., Yang, M.A., Fu, Q., Dupanloup, I., Giampoudakis, K., Nogués-Bravo, D., Rahbek, C., Kroonen, G., Peyrot, M., McColl, H., Vasilyev, S.V., Veselovskaya, E., Gerasimova, M., Pavlova, E.Y., Chasnyk, V.G., Nikolskiy, P.A., Gromov, A.V., Khartanovich, V.I., Moiseyev, V., Grebenyuk, P.S., Fedorchenko, A.Y., Lebedintsev, A.I., Slobodin, S.B., Malyarchuk, B.A., Martiniano, R., Meldgaard, M., Arppe, L., Palo, J.U., Sundell, T., Mannermaa, K., Putkonen, M., Alexandersen, V., Primeau, C., Baimukhanov, N., Malhi, R.S., Sjögren, K.-G., Kristiansen, K., Wessman, A., Sajantila, A., Lahr, M.M., Durbin, R., Nielsen, R., Meltzer, D.J., Excoffier, L., Willerslev, E., 2019. The population history of northeastern Siberia since the Pleistocene. *Nature* 570, 182–188.
Stahler, D.R., MacNulty, D.R., Wayne, R.K., vonHoldt, B., Smith, D.W., 2013. The adaptive value of morphological, behavioural and life-history traits in reproductive female wolves. *The Journal of Animal Ecology* 82, 222–234.
Symes, C.T., Woodborne, S.M., 2010. Trophic level delineation and resource partitioning in a South African afromontane forest bird community using carbon and nitrogen stable isotopes. *African Journal of Ecology*.
Szpak, P., Valenzuela, D., 2020. Camelid husbandry in the Atacama Desert? A stable isotope study of camelid bone collagen and textiles from the Lluta and Camarones Valleys, northern Chile. *PLoS One* 15, e0228332.
Tallian, A., Ciucci, P., Milleret, C., Smith, D., Stahler, D., Wikenros, C., Ordiz, A., 2023. Wolves in a Human World: Social Dynamics of the Northern Hemisphere's Most Iconic Social Carnivore, in: Srinivasan, M., Würsig, B. (Eds.), Social Strategies of Carnivorous Mammalian Predators: Hunting and Surviving as Families. Springer International Publishing, Cham, Switzerland, pp. 89–138.
Tanz, N., Schmidt, H.-L., 2010. δ^{34}S-value measurements in food origin assignments and sulfur isotope

fractionations in plants and animals. *Journal of Agricultural and Food Chemistry* 58, 3139–3146.
Thalmann, O., Perri, A.R., 2019. Paleogenomic Inferences of Dog Domestication, in: Lindqvist, C., Rajora, O.P. (Eds.), Paleogenomics: Genome-Scale Analysis of Ancient DNA, Population Genomics. Springer International Publishing, Cham, Switzerland, pp. 273–306.
Tims, H.W.M., 1896. On the Tooth-genesis in the Canidæ. *Zoological Journal of the Linnean Society* 25, 445–480.
Touzeau, A., Amiot, R., Blichert-Toft, J., Flandrois, J.-P., Fourel, F., Grossi, V., Martineau, F., Richardin, P., Lécuyer, C., 2014. Diet of ancient Egyptians inferred from stable isotope systematics. *Journal of Archaeological Science* 46, 114–124.
Vågene, Å.J., Herbig, A., Campana, M.G., Robles García, N.M., Warinner, C., Sabin, S., Spyrou, M.A., Andrades Valtueña, A., Huson, D., Tuross, N., Bos, K.I., Krause, J., 2018. *Salmonella enterica* genomes from victims of a major sixteenth-century epidemic in Mexico. *Nature Ecology & Evolution* 2, 520–528.
Van den Broeck, M., 2022. Age estimation in puppies and young adult dogs: data driven protocol design for the prevention and detection of age fraud in puppy trade (PhD dissertation). Faculty of Veterinary Medicine, Ghent University. Wachtebeke, University Press.
Van den Broeck, M., De Bels, L., Duchateau, L., Cornillie, P., 2022. Time and sequence of emergence of the deciduous dentition in dogs and its applicability for age estimation. *Anatomia, Histologia, Embryologia* 51, 640–657.
Vydrina, S., Kurbatskiy, V., Polozhiy, A., 1988. Flora Sibiri. Rosaceae vol. 2 (in Russian). *Nauka, Novosibirsk*.
Walter, K.M., Edwards, M.E., Grosse, G., Zimov, S.A., Chapin, F.S., III, 2007. Thermokarst lakes as a source of atmospheric CH_4 during the last deglaciation. *Science* 318, 633–636.
Waples, R.K., Albrechtsen, A., Moltke, I., 2019. Allele frequency-free inference of close familial relationships from genotypes or low-depth sequencing data. *Molecular Ecology* 28, 35–48.
Warinner, C., Korzow Richter, K., Collins, M.J., 2022. Paleoproteomics. *Chemical Reviews* 122, 13401–13446.
Winkler, D.W., Billerman, S.M., Lovette, I.J., 2020. Wagtails and Pipits (Motacillidae), version 1.0. *Birds of the World* Billerman, S.M., Keeney, B.K., Rodewald, P.G. and Schulenberg, T.S. (Eds.). Cornell Lab of Ornithology, Ithaca, NY, USA, https://doi.org/10.2173/bow.motaci1.01.
World Flora Online, 2024. The WFO Plant List https://wfoplantlist.org/.
Yeakel, J.D., Guimarães, P.R., Jr, Bocherens, H., Koch, P.L., 2013. The impact of climate change on the structure of Pleistocene food webs across the mammoth steppe. *Proceedings of the Royal Society B: Biological Sciences* 280, 20130239.
Zeder, M.A., 2015. Core questions in domestication research. *Proceedings of the National Academy of Sciences of the United States of America* 112, 3191–3198.
Zeder, M.A., 2012. The Domestication of Animals. *Journal of Anthropological Research* 68, 161–190.

LIST OF FIGURES

Figure 1: Photos of Tumat-1 (left) and Tumat-2 (right).

Figure 2: Location of the Syalakh site in Siberia. The village of Tumat, after which the canids were originally named, is located 40 km southwest of the Syalakh site. The inset map provides an overview

of the location of the site in northern Asia. Map data are from OpenStreetMap (OpenStreetMap contributors, 2017) and prepared using QGIS (QGIS Development Team, 2023).

Figure 3: Calibrated radiocarbon dates for Tumat-1, Tumat-2 and the mammoth remains found at the Syalakh site. Note that the second date for Tumat-2 is taken from woolly rhinoceros skin found within the canid's GI system. As the Tumat Puppies are expected to be the same age, a posterior distribution of the combined ages was calculated; however, a χ^2-test finds these dates to be in poor agreement. See Supplementary Table 1 for more information.

Figure 4. Plan and stratigraphy of the Syalakh site. A) Overview of the Syalakh site with description of the current landscape. The site is eroding from the eastern side of an oxbow lake next to the Syalakh River. B) Stratigraphic profile of the Syalakh site showing five distinct layers. The Tumat Puppies were found between layers 2 and 3 in the vicinity of the mammoth bone concentration, although due to solifluction of the melting permafrost, the precise location is unknown. Re-ice here refers to subsurface ice that forms in frost cracks by repeated addition of water and subsequent freezing.

Figure 5. 3D images based on CT scans of the skulls and dentition of the Tumat Puppies. A) 3D images of the skulls. B) 3D images of the incompletely calcified crowns of the germs of the lower carnassials (m1). Full lines indicate the length, width or height with measurements given; dotted lines: position of the measurement on the 3D model; ec: entoconid, me: metaconid, hcl: hypoconulid, hy: hypoconid, pa: paraconid, pr: protoconid; not to scale.

Figure 6: Scatter plot of carbon ($\delta^{13}C$) and nitrogen ($\delta^{15}N$) isotope measurements taken from bone collagen of Late Pleistocene animals from northeastern Siberia. Note that the reconstructed values

of the mother of the Tumat Puppies are comparable to measurements of the Ulakhan Sular canid. See Supplementary Table 7 for additional information and results for non-collagen samples.

Figure 7: Identified plant macrofossils found within stomach content of Tumat-1. 1–2: leaves of *Salix* sp.; 3: bud of *Salix* sp.; 4: leaf of *Dryas octopetala*; 5: mosses; 6: spikelet of *Hordeum jubatum*; 7–8: spikelet and seed of *Poa* cf. *arctica*; 9: *Carex* sp. utricle. Scale bar indicates 1 mm.

Figure 8: Results of the kinship analyses. A) READ results indicate that the Tumat Puppies share a full-sibling relationship. The histogram depicts the non-normalized pairwise distance (*P*0) estimated for different groups of canids, with points specifying *P*0 for relevant samples: the Tumat Puppies, three Eurasian grey wolves with a known full-sibling relationship (U1, U2 and U3) and American grey wolves with a known parent-offspring relationship (Yellowstone 2 is the offspring of Yellowstone 1 (mother) and Yellowstone 3 (father)). B) NGSrelate estimates of R_0 and R_1 (top) describe identity-by-state genome-wide sharing patterns between pairs of individuals, while the KING-robust (middle) kinship coefficient measures the overall relatedness of each pair of individuals. In both plots the Tumat Puppies fall near the theoretical expectations for half-siblings, and thus a half-sibling relationship is inferred (abbreviations: FS=full-siblings, HS=half-siblings, PO=parent-offspring and UR=unrelated). NGSrelate estimates of inbreeding coefficients *F* (bottom) indicate the Tumat Puppies have values similar to other Pleistocene wolves and modern Eurasian grey wolves, indicating that these populations provide appropriate comparative datasets for kinship analyses.

ADDITIONAL INFORMATION

Supplementary figures

Supplementary Figure 1: Position of the Tumat-1 find location in relation to where Tumat-2 was excavated in 2015.

Supplementary Figure 2: Photo of Tumat-2 in situ during excavation in 2015.

Supplementary Figure 3: Mammoth bones from the Syalakh site.

Supplementary Figure 4: The right front paw of Tumat-1.

Supplementary Figure 5: Tumat-1 deciduous dentition.

Supplementary Figure 6: The head of Tumat-1.

Supplementary Figure 7: The left paws of Tumat-2.

Supplementary Figure 8: Tumat-2 deciduous dentition.

Supplementary Figure 9: View of the heads of Tumat-1 (left) and Tumat-2 (right).

Supplementary Figure 10: The stomach of Tumat-1 during dissection.

Supplementary Figure 11: Feathers from the stomach of Tumat-1.

Supplementary Figure 12: A piece of skin from the stomach of Tumat-1.

Supplementary Figure 13: The stomach content of Tumat-2 during the partial dissection.

Supplementary Figure 14: Taxonomic distribution of reads assigned with MALT, Tumat-1.

Supplementary Figure 15: Taxonomic distribution of reads assigned with MALT, Tumat-2.

Supplementary Figure 16: Mitochondrial DNA coverage plots of reads mapping to the Sumatran rhinoceros and the woolly rhinoceros.

Supplementary file

Supplementary tables

Supplementary Table 1: Radiocarbon data

Supplementary Table 2: Osteology reference groups

Supplementary Table 3: Milk dentition crown length (CL) comparison

Supplementary Table 4: m1 crown length (CL) comparison

Supplementary Table 5: Isotopic investigation of tissues and stomach content from Tumat-1 and Tumat-2

Supplementary Table 6: Description of the material analysed for Tumat-1 and Tumat-2, the Ulakhan Sular canid, mammoth (*Mammuthus primigenius*), horse (*Equus sp*.), muskox (*Ovibos moschatus*), and cave lion (*Panthera spelaea*) published for northeastern Siberia

Supplementary Table 7: Results of elemental (C, N) and isotopic analysis ($\delta^{13}C$, $\delta^{15}N$) realised on Tumat-1, Tumat-2 and the Ulakhan Sular canid

Supplementary Table 8: Results of elemental (S) and isotopic analysis ($\delta^{34}S$) realised on Tumat-1 and Tumat-2 puppies as well as mammoth (*Mammuthus primigenius*) from the Bykovsky Peninsula

Supplementary Table 9: Samples used in the metagenomic analysis and overview of sequencing output

Supplementary Table 10: Wolf (*Canis lupus*) whole genome and mitochondrial genome

Supplementary Table 11: Whole genome samples used in the kinship analyses

Supplementary Table 12: List of species identified in the MALT analysis.

Supplementary Table 13: Analysis of individual species identified in the metagenomic analyses.

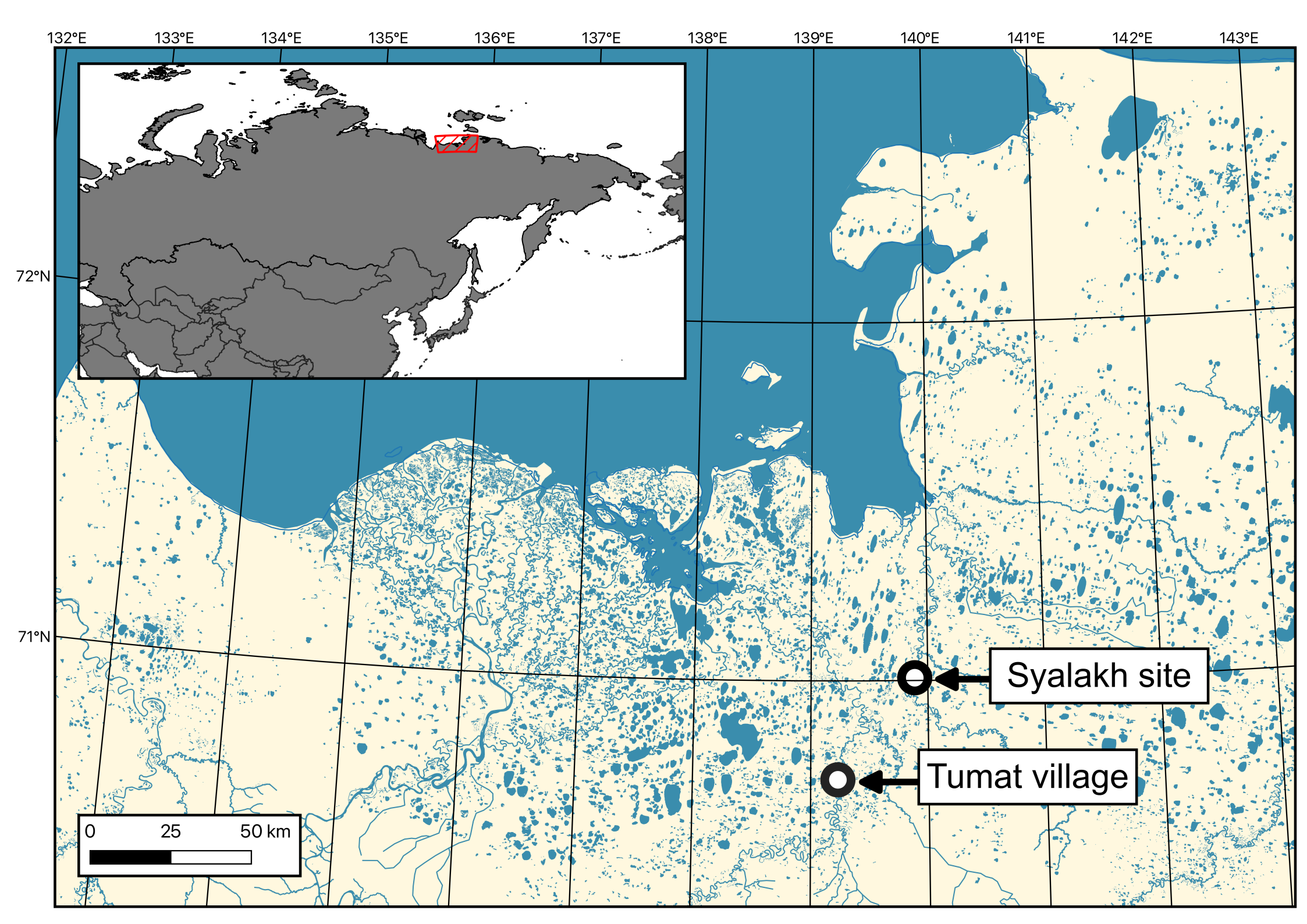
132°E
133°E
134°E
135°E
136°E
137°E
138°E
139°E
140°E
141°E
142°E
143°E
72°N
71°N
Syalakh site
Tumat village
0
25
50 km

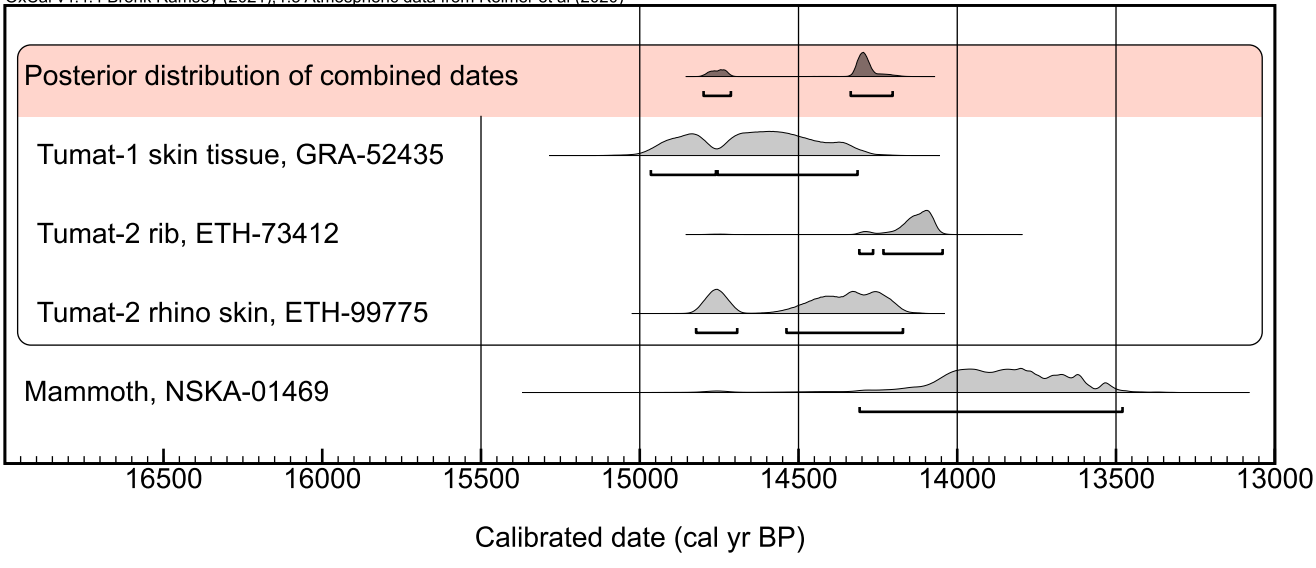
OxCal v4.4.4 Bronk Ramsey (2021); r:5 Atmospheric data from Reimer et al (2020)
Posterior distribution of combined dates
Tumat-1 skin tissue, GRA-52435
Tumat-2 rib, ETH-73412
Tumat-2 rhino skin, ETH-99775
Mammoth, NSKA-01469
16500
16000
15500
15000
14500
14000
13500
13000
Calibrated date (cal yr BP)

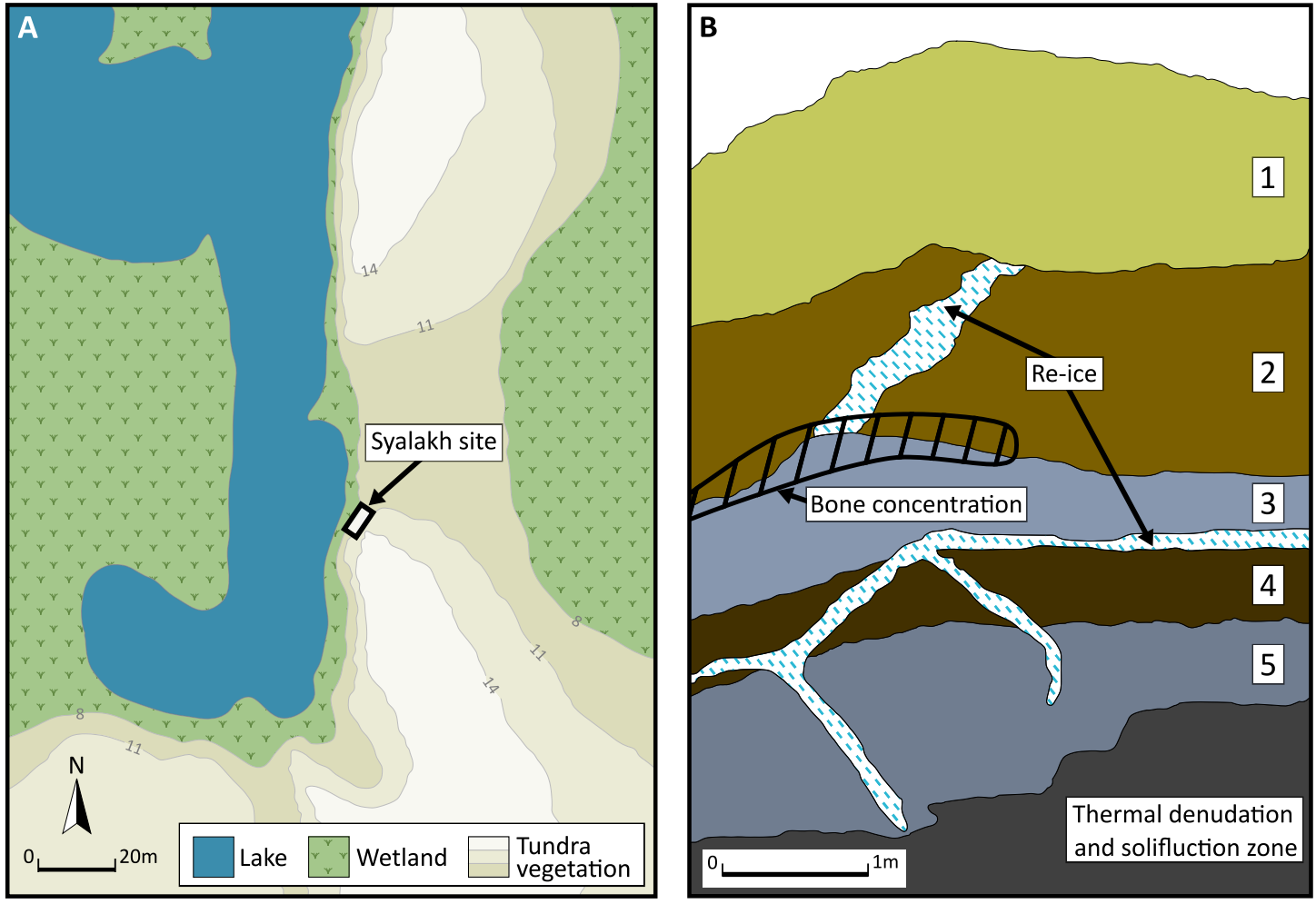
A
14
11
Syalakh site
8
11
14
8
11
N
0
20m
Lake
Wetland
Tundra vegetation
B
1
2
Re-ice
Bone concentration
3
4
5
Thermal denudation and solifluction zone
0
1m

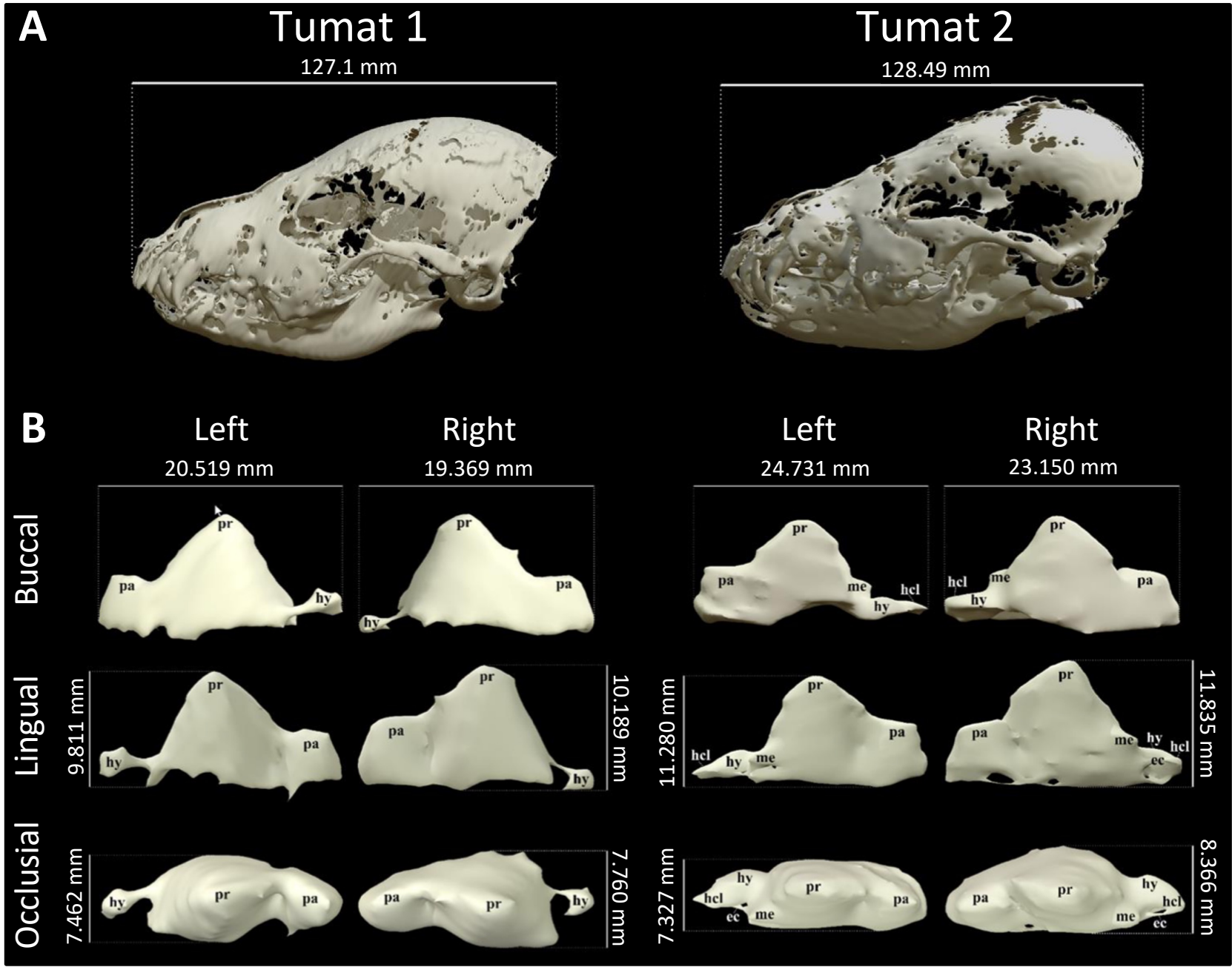
A
Tumat 1
127.1 mm
Tumat 2
128.49 mm
B
Left
20.519 mm
Right
19.369 mm
Left
24.731 mm
Right
23.150 mm
Buccal
Lingual
Occlusial
9.811 mm
10.189 mm
11.280 mm
11.835 mm
7.462 mm
7.760 mm
7.327 mm
8.366 mm
pr
pa
hy
hcl
me
ec

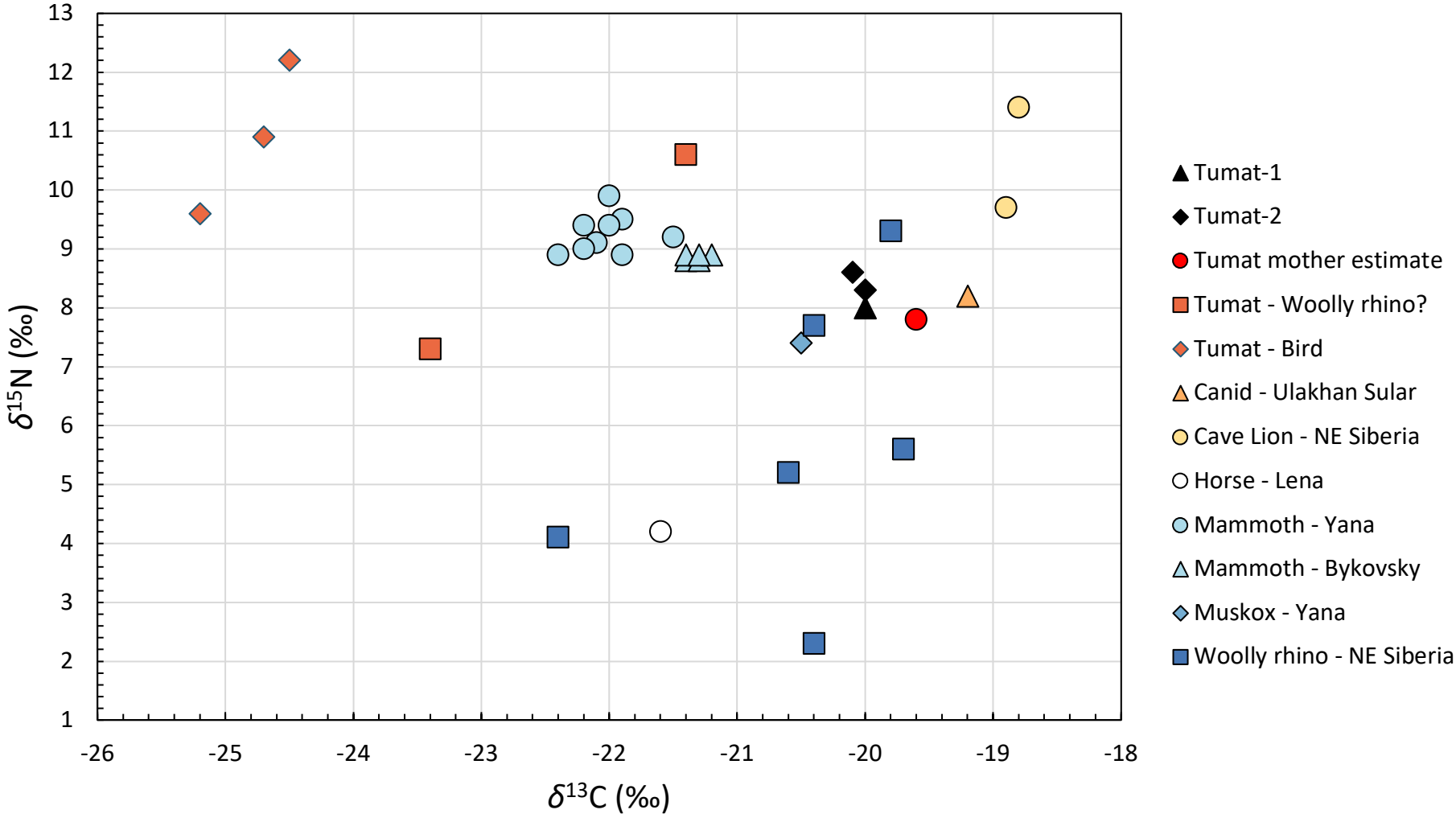
13
12
11
10
9
8
7
6
5
4
3
2
1
δ15N (‰)
-26
-25
-24
-23
-22
-21
-20
-19
-18
δ13C (‰)
Tumat-1
Tumat-2
Tumat mother estimate
Tumat - Woolly rhino?
Tumat - Bird
Canid - Ulakhan Sular
Cave Lion - NE Siberia
Horse - Lena
Mammoth - Yana
Mammoth - Bykovsky
Muskox - Yana
Woolly rhino - NE Siberia

1
2
3
4
5
6
7
8
9
1 mm

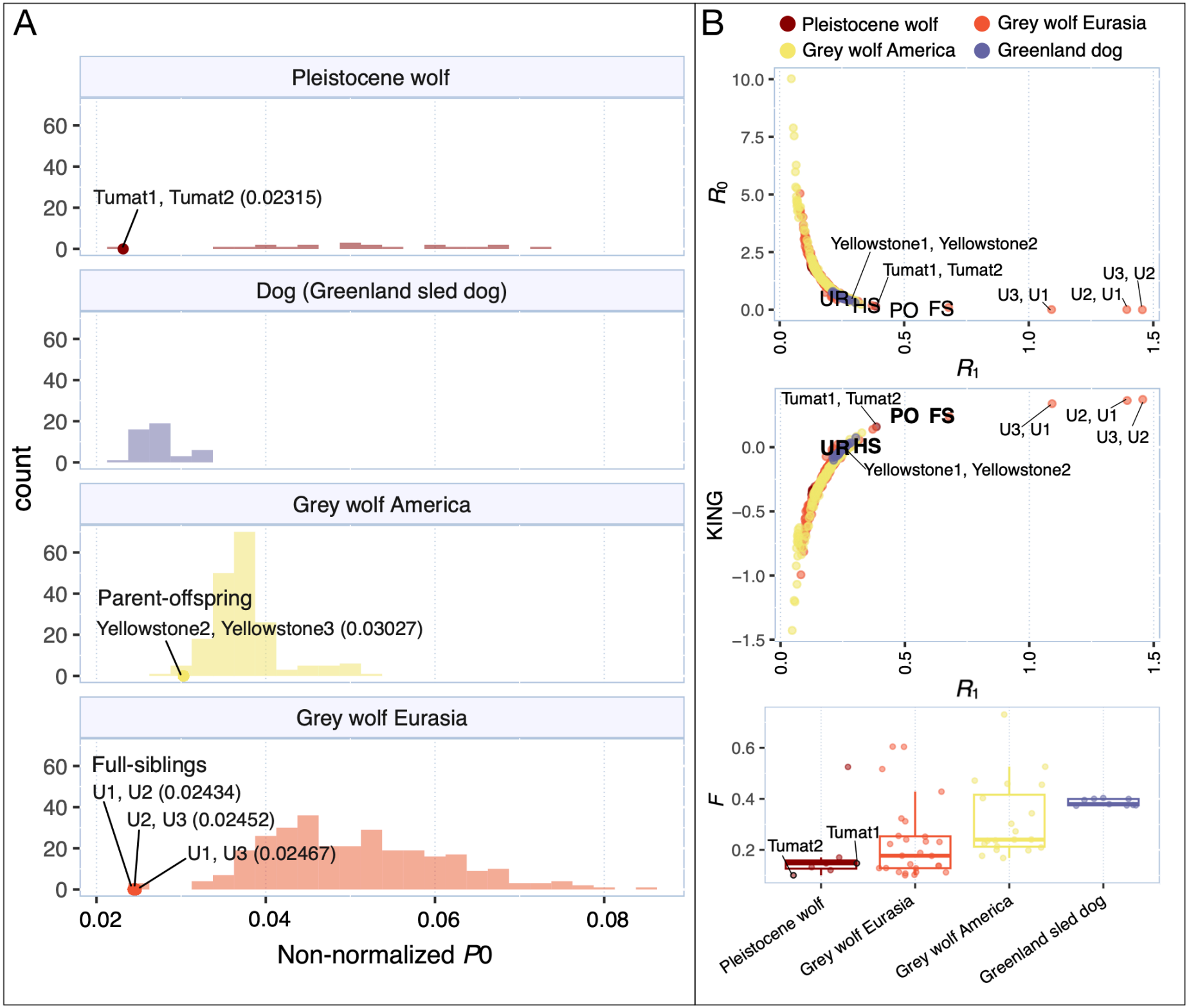
A
Pleistocene wolf
Tumat1, Tumat2 (0.02315)
Dog (Greenland sled dog)
Grey wolf America
Parent-offspring
Yellowstone2, Yellowstone3 (0.03027)
Grey wolf Eurasia
Full-siblings
U1, U2 (0.02434)
U2, U3 (0.02452)
U1, U3 (0.02467)
count
Non-normalized P0
B
Pleistocene wolf
Grey wolf Eurasia
Grey wolf America
Greenland dog
R0
R1
Yellowstone1, Yellowstone2
Tumat1, Tumat2
U3, U2
U3, U1
U2, U1
UR HS PO FS
KING
F
Tumat2
Tumat1
Pleistocene wolf
Grey wolf Eurasia
Grey wolf America
Greenland sled dog

Multifaceted analysis reveals diet and kinship of Late Pleistocene “Tumat Puppies”: Supplementary figures

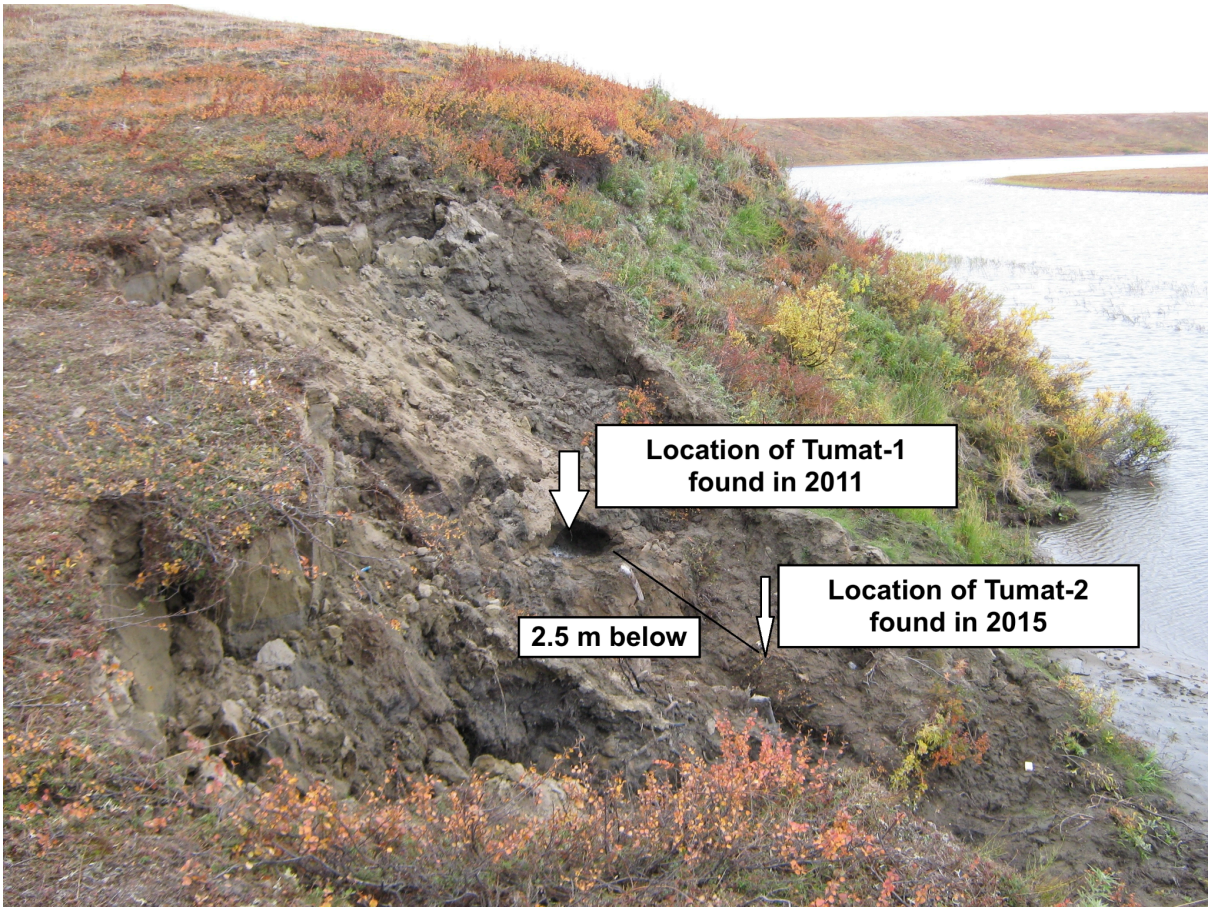

Supplementary Figure 1: Position of the Tumat-1 find location in relation to where Tumat-2 was excavated in 2015. Note that there had been a landslide in the years between the discovery of Tumat-1 and the excavation that uncovered Tumat-2.

Supplementary Figure 2: Photo of Tumat-2 in situ during excavation in 2015.

Supplementary Figure 3: Mammoth bones from the Syalakh site. Bones have indications of both human processing, as well as natural fragmentation. Top: burned bone. The bottom three have straight edges, indicative of cutting in prehistory. Bottom rib has an example of a potential natural break on the left side.

Supplementary Figure 4: The right front paw of Tumat-1. Pale hairs are visible.

Supplementary Figure 5: Tumat-1 deciduous dentition.

Supplementary Figure 6: The head of Tumat-1. Downy fur and left ear is visible.

Supplementary Figure 7: The left paws of Tumat-2. Pale hairs are visible.

Supplementary Figure 8: Tumat-2 deciduous dentition.

Supplementary Figure 9: View of the heads of Tumat-1 (left) and Tumat-2 (right).

Supplementary Figure 10: The stomach of Tumat-1 during dissection. The stomach lining is cut open and folded back, revealing the stomach content.

Supplementary Figure 11: Feathers from the stomach of Tumat-1. DNA was extracted from the tissue as metagenomic subsample T1:S4

Supplementary Figure 12: A piece of skin from the stomach of Tumat-1. DNA was extracted from the tissue as metagenomic subsample T1:S5. A subsample of this was also included in Lord et al. (2020) and revealed to have originated from woolly rhinoceros.

Supplementary Figure 13: The stomach content of Tumat-2 during the partial dissection. The light grey colour of the stomach content is clearly visible.

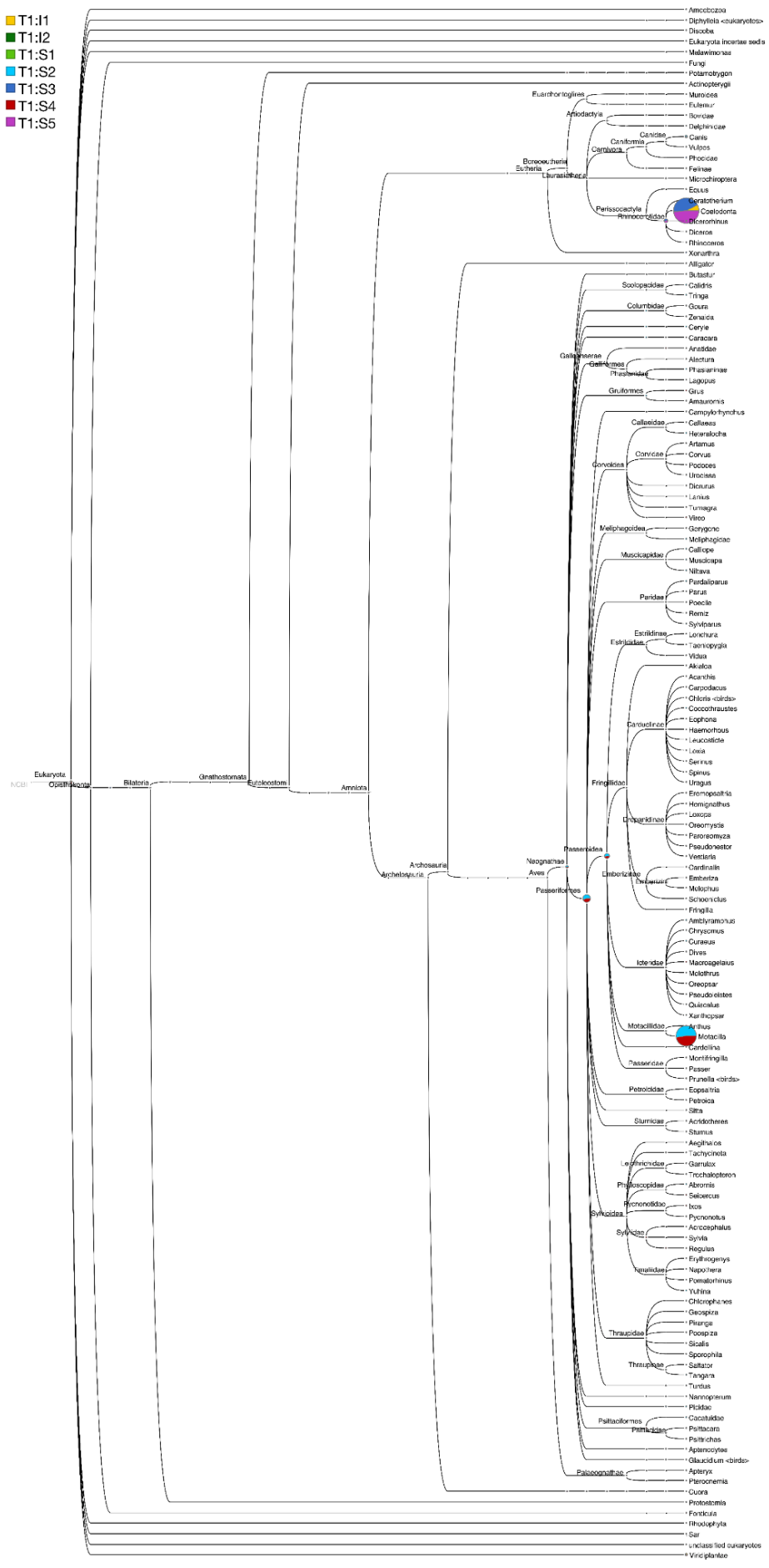
T1:I1
T1:I2
T1:S1
T1:S2
T1:S3
T1:S4
T1:S5
NCBI
Eukaryota
Opisthokonta
Bilateria
Gnathostomata
Euteleostomi
Amniota
Archosauria
Archelosauria
Neognathae
Aves
Passeriformes
Passeroidea
Fringillidae
Emberizidae
Cardueliinae
Carduelinae
Motacillidae
Passeridae
Petroicidae
Sturnidae
Sylviidae
Thraupidae
Psittaciformes
Palaeognathae
Euarchontoglires
Artiodactyla
Boreoeutheria
Eutheria
Laurasiatheria
Perissodactyla
Rhinocerotidae
Canidae
Caniformia
Carnivora
Cervoidea
Galloanserae
Galliformes
Phasianidae
Gruiformes
Callaeidae
Corvidae
Meliphagoidea
Muscicapidae
Paridae
Estrildinae
Estrildidae
Emberizidae
Icteridae
Motacillidae
Passeridae
Petroicidae
Sturnidae
Sylviidae
Thraupidae
Psittaciformes
Palaeognathae
Amoebozoa
Diphyllela <eukaryotes>
Discoba
Eukaryota incertae sedis
Melawimonas
Fungi
Potamotrygon
Actinopterygii
Muroidea
Eulemur
Bovidae
Delphinidae
Canis
Vulpes
Phocidae
Felinae
Microchiroptera
Equus
Ceratotherium
Coelodonta
Dicerorhinus
Diceros
Rhinoceros
Xenarthra
Alligator
Bubastur
Calidris
Tringa
Goura
Zenaida
Ceryle
Caracara
Anatidae
Alectura
Phasianinae
Lagopus
Grus
Amaurornis
Campylorhynchus
Callaeas
Heteralocha
Artamus
Corvus
Pococes
Urocissa
Dicrurus
Lanius
Turnagra
Vireo
Gerygone
Meliphagidae
Calliope
Muscicapa
Niltava
Pardaliparus
Parus
Poecile
Remiz
Sylviparus
Lonchura
Taeniopygia
Vidua
Akialoa
Acanthis
Carpodacus
Chloris <birds>
Coccothraustes
Eophona
Haemorhous
Leucosticte
Loxia
Serinus
Spinus
Uragus
Eremopsaltria
Hemignathus
Loxops
Oreomystis
Paroreomyza
Pseudonestor
Vestiaria
Cardinalis
Emberiza
Melophus
Schoeniclus
Fringilla
Amblyramphus
Chrysomus
Curaeus
Dives
Macroagelaius
Molothrus
Oreopsar
Pseudoleistes
Quiscalus
Xanthopsar
Anthus
Motacilla
Cardellina
Montifringilla
Passer
Prunella <birds>
Eopsaltria
Petroica
Sitta
Acridotheres
Sturnus
Aegithalos
Tachycineta
Garrulax
Trochalopteron
Abromis
Seicercus
Ixos
Pycnonotus
Acrocephalus
Sylvia
Regulus
Erythrogenys
Napothera
Pomatorhinus
Yuhina
Chlorophanes
Geospiza
Piranga
Poospiza
Sicalis
Sporophila
Saltator
Tangara
Turdus
Nannopterum
Picidae
Cacatuidae
Psittacara
Psittrichas
Aptenocytes
Glaucidium <birds>
Apteryx
Pterocnemia
Cuora
Protostomia
Fonticula
Rhodophyta
Sar
unclassified eukaryotes
Viridiplantae

Supplementary Figure 14: Taxonomic distribution of reads assigned with MALT, Tumat-1. Analysis was performed in MEGAN at genus level. Each colour corresponds to a different subsample from the GI tract, see Table S9 for information about the sample type.

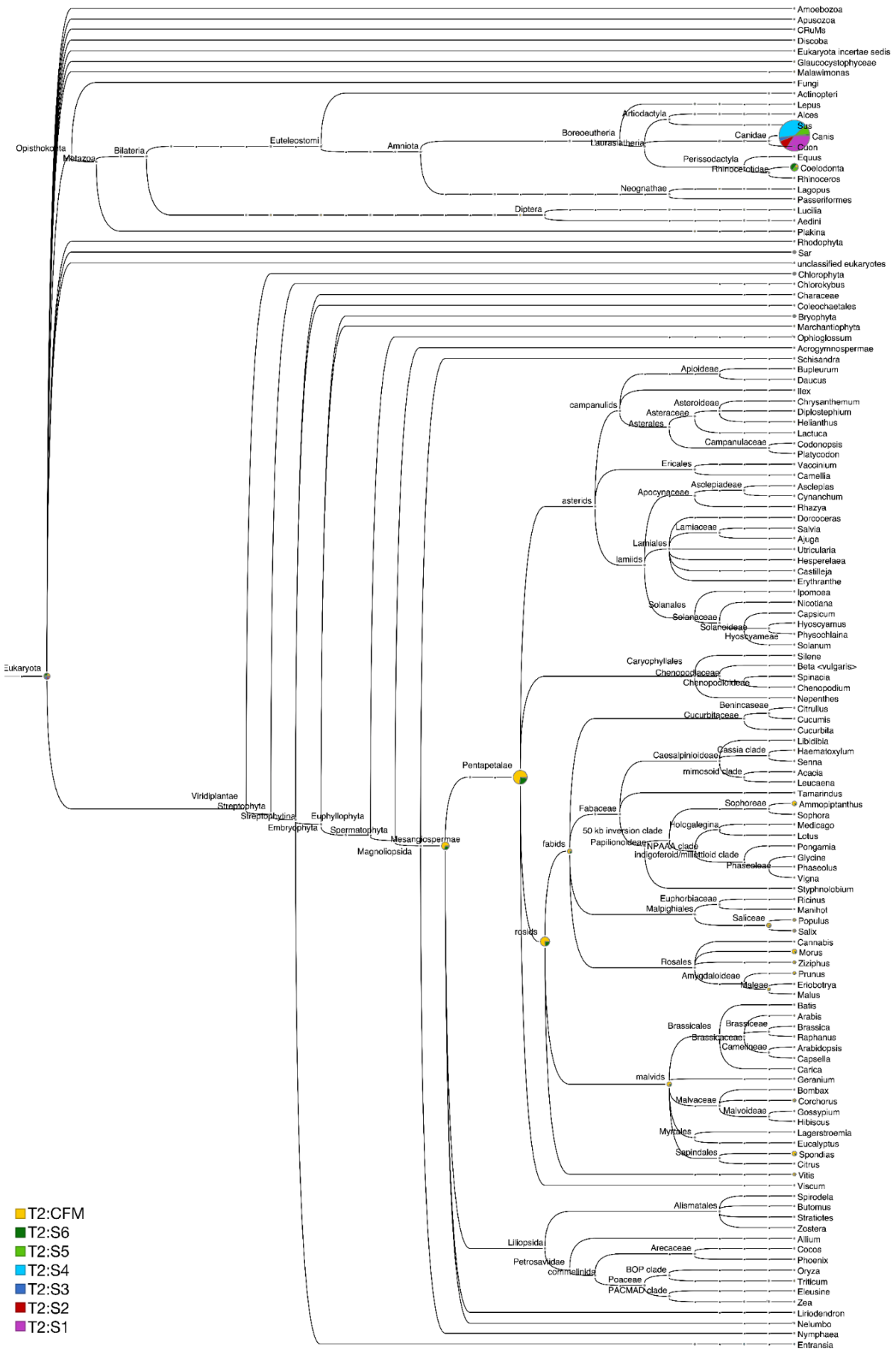
Amoebozoa
Apusozoa
CRuMs
Discoba
Eukaryota incertae sedis
Glaucocystophyceae
Malawimonas
Fungi
Actinopteri
Lepus
Alces
Sus
Canis
Dolichotis
Equus
Coelodonta
Rhinoceros
Lagopus
Passeriformes
Lucilia
Aedini
Plakina
Rhodophyta
Sar
unclassified eukaryotes
Chlorophyta
Chlorokybus
Characeae
Coleochaetales
Bryophyta
Marchantiophyta
Ophioglossum
Acrogymnospermae
Schisandra
Bupleurum
Daucus
Ilex
Chrysanthemum
Diplostephium
Helianthus
Lactuca
Codonopsis
Platycodon
Vaccinium
Camellia
Asclepias
Cynanchum
Rhazya
Dorcoceras
Salvia
Ajuga
Utricularia
Hesperelaea
Castilleja
Erythranthe
Ipomoea
Nicotiana
Capsicum
Hyoscyamus
Physochlaina
Solanum
Silene
Beta <vulgaris>
Spinacia
Chenopodium
Nepenthes
Citrullus
Cucumis
Cucurbita
Libidibia
Haematoxylum
Senna
Acacia
Leucaena
Tamarindus
Ammopiptanthus
Sophora
Medicago
Lotus
Pongamia
Glycine
Phaseolus
Vigna
Styphnolobium
Ricinus
Manihot
Populus
Salix
Cannabis
Morus
Ziziphus
Prunus
Eriobotrya
Malus
Batis
Arabis
Brassica
Raphanus
Arabidopsis
Capsella
Carica
Geranium
Bombax
Corchorus
Gossypium
Hibiscus
Lagerstroemia
Eucalyptus
Spondias
Citrus
Vitis
Viscum
Spirodela
Butomus
Stratiotes
Zostera
Allium
Cocos
Phoenix
Oryza
Triticum
Eleusine
Zea
Liriodendron
Nelumbo
Nymphaea
Entransia
campanulids
Apioideae
Asteroideae
Asteraceae
Asterales
Campanulaceae
asterids
Ericales
Asclepiadeae
Apocynaceae
Lamiaceae
Lamiales
lamiids
Solanales
Solanaceae
Solanoideae
Hyoscyameae
Caryophyllales
Chenopodiaceae
Chenopodioideae
Benincaseae
Cucurbitaceae
Caesalpinioideae
Cassia clade
mimosoid clade
Fabaceae
Sophoreae
50 kb inversion clade
Papilionoideae
Hologalegina
NPAAA clade
Indigoferoid/millettioid clade
Phaseoleae
fabids
Euphorbiaceae
Malpighiales
Saliceae
rosids
Rosales
Amygdaloideae
Maleae
Brassicales
Brassicaceae
Brassicaceae
Cameleae
malvids
Malvaceae
Malvoideae
Myrtales
Sapindales
Pentapetalae
Alismatales
Liliopsida
Petrosaviidae
commelinids
Arecaceae
BOP clade
Poaceae
PACMAD clade
Mesangiospermae
Magnoliopsida
Spermatophyta
Euphyllophyta
Streptophytina
Streptophyta
Viridiplantae
Embryophyta
Eukaryota
Opisthokonta
Metazoa
Bilateria
Euteleostomi
Amniota
Boreoeutheria
Laurasiatheria
Artiodactyla
Canidae
Perissodactyla
Rhinocerotidae
Neognathae
Diptera
T2:CFM
T2:S6
T2:S5
T2:S4
T2:S3
T2:S2
T2:S1

Supplementary Figure 15: Taxonomic distribution of reads assigned with MALT, Tumat-2. Analysis was performed in MEGAN at genus level. Each colour corresponds to a different subsample from the GI tract, see Table S9 for information about the sample type.

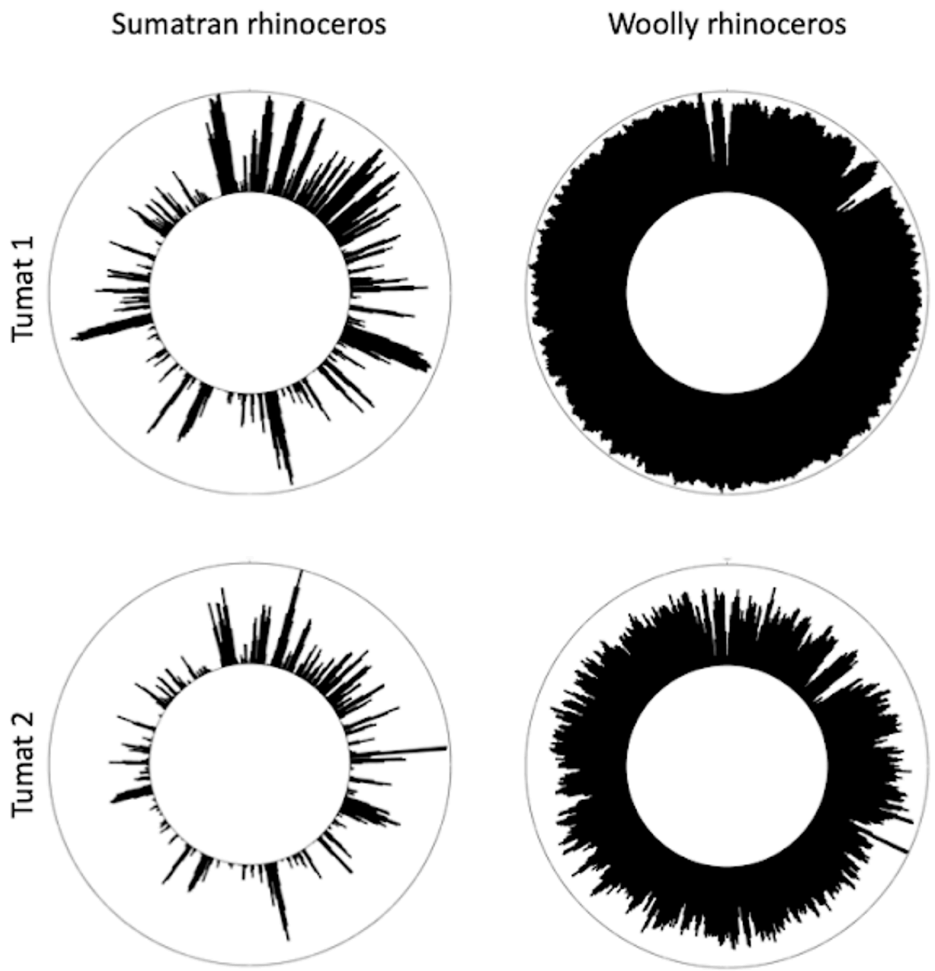

Supplementary Figure 16: Mitochondrial DNA coverage plots of reads mapping to the Sumatran rhinoceros and the woolly rhinoceros. The Sumatran rhinoceros is the closest living relative of the woolly rhinoceros. The plots depict the combined data from the seven subsamples from each of the Tumat Puppies. Note that the length of bars is not to scale, but only to illustrate the coverage for the different species at any one site.